Optimizing solar-powered multi-generation systems for sustainable energy management in university buildings using Neural Networks and Genetic Algorithms

Journal of Building Engineering 108 (2025) 112939

Contents lists available at ScienceDirect

Journal of Building Engineering

journal homepage: www.elsevier.com/locate/jobe

Optimizing solar-powered multi-generation systems for sustainable energy management in university buildings using Neural Networks and Genetic Algorithms

Ehsanolah Assareh [a,b,c,1,*], Nima Izadyar [b,d,1,**], Elmira Jamei [b,d], Mohammad amin Monzavian [c], Saurabh Agarwal [e,1], Neha Agarwal [f,1]

[a] Strategic Research Institute (SRI), Asia Pacific University of Technology and Innovation (APU), Technology Park Malaysia, Kuala Lumpur, Malaysia
[b] Built Environment and Engineering Program, College of Sport, Health and Engineering (CoSHE), Victoria University, Melbourne, Australia
[c] Department of Renewable Energy Technology, Materials and Energy Research Center, Dezful Branch, Islamic Azad University, Dezful, Iran
[d] Institute for Sustainable Industries and Liveable Cities, Victoria University, Melbourne, VIC, 3011, Australia
[e] School of Computer Science and Engineering, Yeungnam University, Gyeongsan, 38541, South Korea
[f] School of Chemical Engineering, Yeungnam University, Gyeongsan, 38541, South Korea

ARTICLE INFO

Keywords:
Artificial intelligence optimization
Energy efficiency
Renewable energy integration
Solar-powered multi-generation systems
Sustainable university campuses

ABSTRACT

University campuses operate like small cities, with complex energy demands driven by diverse activities, making energy management particularly challenging in extreme climates. Traditional energy systems often rely on fossil fuels, leading to inefficiencies, high costs, and increased carbon footprints. This study optimizes a solar-powered multi-generation system for a university building in the severe hot climate of Dezful, Iran, using a two-step approach. First, the Building Energy Optimization Tool (BEopt) was used to select optimal building materials, leading to a reduction in total energy demand. Then, Artificial Intelligence algorithms (Neural Networks and Genetic Algorithms) were applied to enhance system performance and cost-effectiveness. The Engineering Equation Solver (EES) validated the thermodynamic performance of the optimized system. This optimized system generates 49.55 GW-hours (GWh) of electricity annually, along with 19.47 GWh of heating and 13.93 GWh of cooling, producing a surplus of 34.28 GWh (69 % of total generation). Compared to the base case, electricity generation increased by over 224 %, cooling by 120 %, and heating by more than 3500 %, while CO_2 emissions decreased from 37.18 to 35.34 metric tons/year. The optimized system operates with an exergy efficiency of 23.44 % and a cost rate of 14.93 $/h. What sets this study novel is the integration of demand-side improvements with AI-enhanced multi-generation systems and thermodynamic validation, creating a practical model for achieving net-zero energy on university campuses. This methodology is scalable to more complex energy networks, including district energy systems, with future work focusing on real-time weather integration and advanced forecasting to improve adaptability and resilience.

* Corresponding author. Built Environment and Engineering Program, College of Sport, Health and Engineering (CoSHE), Victoria University, Melbourne, Australia.
** Corresponding author. Built Environment and Engineering Program, College of Sport, Health and Engineering (CoSHE), Victoria University, Melbourne, Australia.
E-mail addresses: ehsanolah.assareh@vu.edu.au (E. Assareh), nima.izadyar@vu.edu.au (N. Izadyar).
[1] These authors contributed equally to this article as the first authors.

https://doi.org/10.1016/j.jobe.2025.112939
Received 7 March 2025; Received in revised form 6 May 2025; Accepted 15 May 2025
Available online 17 May 2025

Nomenclature

Abbreviations	Definition/Unit
AI	Artificial Intelligence
ANNs	Artificial Neural Networks
BEopt	Building Energy Optimization Tool
CO_2	Carbon Dioxide (metric tons/year)
EES	Engineering Equation Solver
GAs	Genetic Algorithms
GHI	Global Horizontal Irradiation (W/m^2)
LCC	Life Cycle Cost ($)
NPV	Net Present Value ($)
PV	Photovoltaic
ZEB	Zero Energy Buildings
Symbol	**Definition/Unit**
A	Area of the collector surface (m^2)
b	PV collector width parameter (m^{-1})
B_C	Width of collector surface
C_{air}	Specific heat of air
g	Gravitational acceleration (m/s^2)
GB	Solar beam radiation (W/m^2)
h_i, h_e	Inlet/outlet specific enthalpy (kJ/kg)
h_{p2}	Heat transfer coefficient (second stage), (W/m^2.K)
L	PV panel length (m)
$\dot{m}_i, \dot{m}_e$	Inlet/outlet mass flow rate (kg/s)
$\dot{m}_{air}$	Air mass flow rate (kg/s)
P_0	Ambient pressure (kPa)
$\dot{Q}$	Heat transfer rate into the control volume (kW)
$\dot{Q}_{PV}$	Useful thermal energy output of PV system (kW)
$T_{air,in}$	Inlet air temperature (°C)
T_0	Ambient temperature (°C)
U_l	Overall heat transfer coefficient (W/m^2.K)
v_i, v_e	Inlet/outlet velocity (m/s)
$\dot{W}$	Work output from the control volume
W_{PV}	Power generated by PV panels (kW)
η_C	Conversion efficiency of PV module (−)
P_0	Ambient pressure (kPa)
Z	Elevation
Z_i, Z_e	Inlet/outlet elevation (m)
Greek symbol	**Definition/Unit**
φ	Maintenance factor
η	Efficiency [−]
σ	Stefan–Boltzmann constant [W/m^2.K^4]

1. Introduction

As cities grow and buildings become more complex, global energy demand has been rising sharply, especially with the growing use of energy-intensive technologies [1,2]. This demand surge is often paired with difficulties in achieving sustainability goals, particularly in lower- and middle-income countries [3,4]. Moreover, stricter energy regulations now require buildings, especially older structures, to undergo substantial retrofitting to improve energy performance and meet sustainability targets [5,6]. Among these, university campuses stand out as major energy consumers due to their continuous operations across diverse spaces (e.g., laboratories, offices, and communal areas) with varying energy demands [7–9]. The literature highlights that research facilities within university campuses account for a substantial share of total campus energy consumption due to their intensive operational requirements [10], with some studies estimating this share to be approximately 40 % [11]. However, managing energy use in these institutions is complicated by aging infrastructure [12,13], characterized by outdated design, inefficient building envelopes, and limited integration of renewable energy technologies, significantly restricting their adaptability to modern efficiency standards [14,15]. Such limitations highlight the need for energy-efficient retrofitting and renewable energy integration to effectively reduce demand, operational costs, carbon emissions, and reliance on fossil fuels [16–18].

Given these challenges related to aging infrastructure and limited renewable integration, dependence solely on conventional energy sources is increasingly inadequate for meeting sustainability goals. Consequently, transitioning toward more integrated, self-sufficient solutions, such as Zero Energy Buildings (ZEB), has become essential [19,20]. ZEB systems balance their energy consumption with on-site renewable energy generation, achieving net-zero carbon emissions [21–24]. Among various renewable energy sources, solar power stands out as a choice due to its wide availability, scalability, and ability to generate clean energy on-site, making it particularly effective in regions with abundant solar radiation year-round [25–28]. For instance, a solar-based multi-generation system achieved notable energy (13.93 % and 14.1 %) and exergy efficiencies (11.18 % and 10.93 %) under real climatic conditions in the severe hot climates of Doha and Bushehr [29]. Another study demonstrated the feasibility of a flexible solar-hydrogen multi-generation system operating effectively across Iran's diverse climates, showing the highest exergy efficiency (26.3 %) and lowest cost rate ($6.08/h) in Bandar Abbas, underscoring the adaptability and environmental benefits of such systems in varied weather contexts [30]. To support ZEB objectives, solar-powered multi-generation systems, capable of simultaneously providing cooling, thermal energy, and electricity, have gained popularity as versatile solutions [31–35], even for large-scale and energy-intensive environments [36,37]. These systems hold excellent potential for minimizing environmental impact, particularly in university campuses [38,39]. For example, one study reported a CO_2 reduction of 2026.5 metric tons/year [37]. Nonetheless, relying on a single renewable source may not guarantee a stable energy supply, particularly during periods of reduced solar output. Therefore, adopting a holistic approach that emphasizes demand-side efficiency and optimized multi-generation systems performance is critical [40–42]. In this context, advancements in energy modeling and Artificial Intelligence (AI) present valuable strategies for enhancing energy performance, improving system resilience, and facilitating renewable energy integration, thereby promoting cost-effective and sustainable energy management.

To operate such integrated renewable solutions, advanced energy modeling and optimization tools are critical in accurately predicting building performance, guiding effective strategies for both demand reduction and renewable energy integration. Regarding energy modeling, previous studies have explored various approaches to enhance building energy performance, with a strong emphasis on reducing heating and cooling loads while improving efficiency, cost-effectiveness, and sustainability [38,43,44]. For example, a reliable model was developed using Artificial Neural Networks (ANNs) trained on a dataset of 12,960 simulated residential building scenarios, demonstrating 98 % accuracy in estimating annual cooling loads at the early design stage [45]. Simulation-based approaches using software such as EnergyPlus, TRNSYS, and the Building Energy Optimization Tool (BEopt) have been widely employed

to analyze energy consumption patterns and optimize building performance [46,47]. Among these tools, BEopt has been particularly effective for whole-building energy performance assessment [48,49], as it utilizes a steady-state modeling approach that simplifies computations while maintaining accuracy in evaluating strategies. Unlike EnergyPlus and TRNSYS, which focus on detailed transient simulations and dynamic load analyses [50,51] with higher correlations with hourly measurements [52], BEopt streamlines the optimization process by balancing computational efficiency with practical design insights, making it particularly suited for early-stage energy assessments and demand-side management [53,54]. While modeling software, like BEopt, effectively optimizes demand-side energy performance by reducing building loads and improving efficiency, achieving a well-balanced and resilient energy system requires a complementary approach that evaluates thermodynamic behavior and multi-generation system performance [55,56]. As an example, a solar-driven multi-generation system for a university campus was optimized using a combination of building energy simulation (BEopt), thermodynamic analysis via the Engineering Equation Solver (EES), a tool widely employed to optimize energy distribution and balance power, heating, and cooling loads [55,57,58], and machine learning-based multi-objective optimization targeting exergy efficiency and cost [59]. This integrated approach achieved an exergy efficiency of 25.69 % and a cost of $10.15/h, demonstrating how coupling BEopt-driven demand reduction with EES-based thermodynamic modeling provides a robust energy strategy that reduces consumption while improving system reliability and cost-effectiveness [59]. Together, these tools enable more informed and integrated energy planning for high-performance buildings.

Building on this integrated modeling foundation, recent studies have increasingly incorporated AI-based multi-objective optimization techniques, such as ANNs and Genetic Algorithms (GAs), to improve efficiency, lower costs, and reduce CO_2 emissions [60–63]. Past research shows that AI-based optimization has significantly boosted both energy and exergy efficiency in Refs. [58,64,65], lowered cost rates [30,66], and reduced CO_2 emissions by thousands of metric tons/year [30,58,67]. ANNs are particularly effective in capturing complex, non-linear energy system behaviors [68], optimizing energy generation under varying conditions [66,69,70], while GAs excel in exploring large solution spaces and identifying optimal configurations for systems with multiple objectives [71–73]. For instance, in a recent study, a multi-generation system integrated with a desalination unit for a smart building was thermodynamically analyzed and optimized, achieving an energy efficiency of 46.66 % and a cost of purified water of $\$4.49/m^3$, using ANN-based demand prediction and Genetic Algorithm optimization [74]. Similarly, another study employed ANN-based thermodynamic and thermoeconomic modeling combined with GA optimization to enhance a solar–geothermal cogeneration system, achieving 43.5 % exergy efficiency, boosting net power and cooling capacities, and reducing electricity and cooling costs by 12.1 % and 41.9 % [60]. Given the potential of these AI techniques, integrating GA and ANN with BEopt for demand-side energy reduction and EES for multi-generation system analysis can offer a resilient, cost-effective, and sustainable energy management framework. Yet, most studies treat demand reduction and system optimization separately, lacking a unified approach, critical for energy-intensive settings like university campuses.

To address this research gap, this study presents a unified optimization framework that integrates these previously isolated methodologies. It applies AI-driven optimization to a real-world case study of a university building in Dezful, Iran, aiming to maximize system efficiency, reduce costs, and ensure resilience. A hybrid approach combining demand-side optimization (BEopt), thermodynamic analysis (EES), and AI-based optimization (GA and ANN) is implemented to enhance system performance. The novelty lies in integrating multi-objective AI optimization with thermodynamic validation, bridging demand-side and supply-side strategies to develop a scalable, data-driven framework for achieving net-zero energy in educational institutions. Although the case study is set in a hot climate, the methodology is adaptable to buildings with varying thermal properties and climates. By retraining the neural network with site-specific building data, climatic variables, and occupancy profiles, the system can be customized for broader applications. This flexibility supports implementation across temperate, cold, or mixed climates. This paper is structured as follows: Section 2 outlines the methodology, including optimization techniques, simulation tools, and analytical approaches. Section 3 describes the system design and optimization, with validation. Section 4 presents results and discussion. Section 5 outlines study limitations and future directions. Section 6 concludes with key findings and their implications for achieving net-zero energy in educational institutions.

2. Methodology

This section describes the utilized methodology, which consists of demand-side optimization (Section 2.1), supply-side optimization (Section 2.2), and the overall research framework (Section 2.3).

2.1. Demand-side optimization

The demand-side optimization focuses on minimizing the building's energy loads through envelope and material improvements before integrating renewable energy systems. BEopt is used to simulate building energy performance under local climate conditions (sourced from Meteonorm [75]), while EES is employed to complement BEopt by validating the thermodynamic accuracy of simulated loads. EES applied first-law energy balance calculations to verify and refine heating, cooling, and power demands, enhancing the accuracy of BEopt's steady-state results. Key steps include:

1. **Energy Load Calculation:** BEopt is used to simulate annual building energy demand, while EES refines these results by evaluating instantaneous power needs and validating thermal behavior based on building envelope characteristics.
2. **Material Optimization:** BEopt is used to run parametric analyses in order to identify high-performance envelope materials, while EES verifies the corresponding reductions in peak loads.

3. **Performance Comparison:** The optimized design is benchmarked against the baseline case to quantify improvements in cooling, heating, and electricity demand.

This process generates a validated and thermodynamically consistent demand profile that serves as the input for the supply-side system modeling and AI-driven optimization.

2.2. Supply-side optimization

The supply-side analysis models and optimizes a solar-powered multi-generation system to meet the optimized building's energy demand. EES is used to build a detailed thermodynamic model of the system, incorporating climatic data from Meteonorm to simulate performance under realistic climate conditions. The system includes components such as Photovoltaic (PV) panels and condensing chillers to provide electricity, heating, and cooling. To identify the most effective system configurations, a hybrid optimization framework is applied using AI, integrating ANNs and GAs, to efficiently explore the complex, non-linear design space. Key steps include:

1. **Thermodynamic Modeling in EES:** EES simulates the thermodynamic performance of the multi-generation system across a range of design configurations. This includes calculating electricity generation, thermal output, and overall system efficiency based on PV area, orientation, thermal collector size, and other design variables.

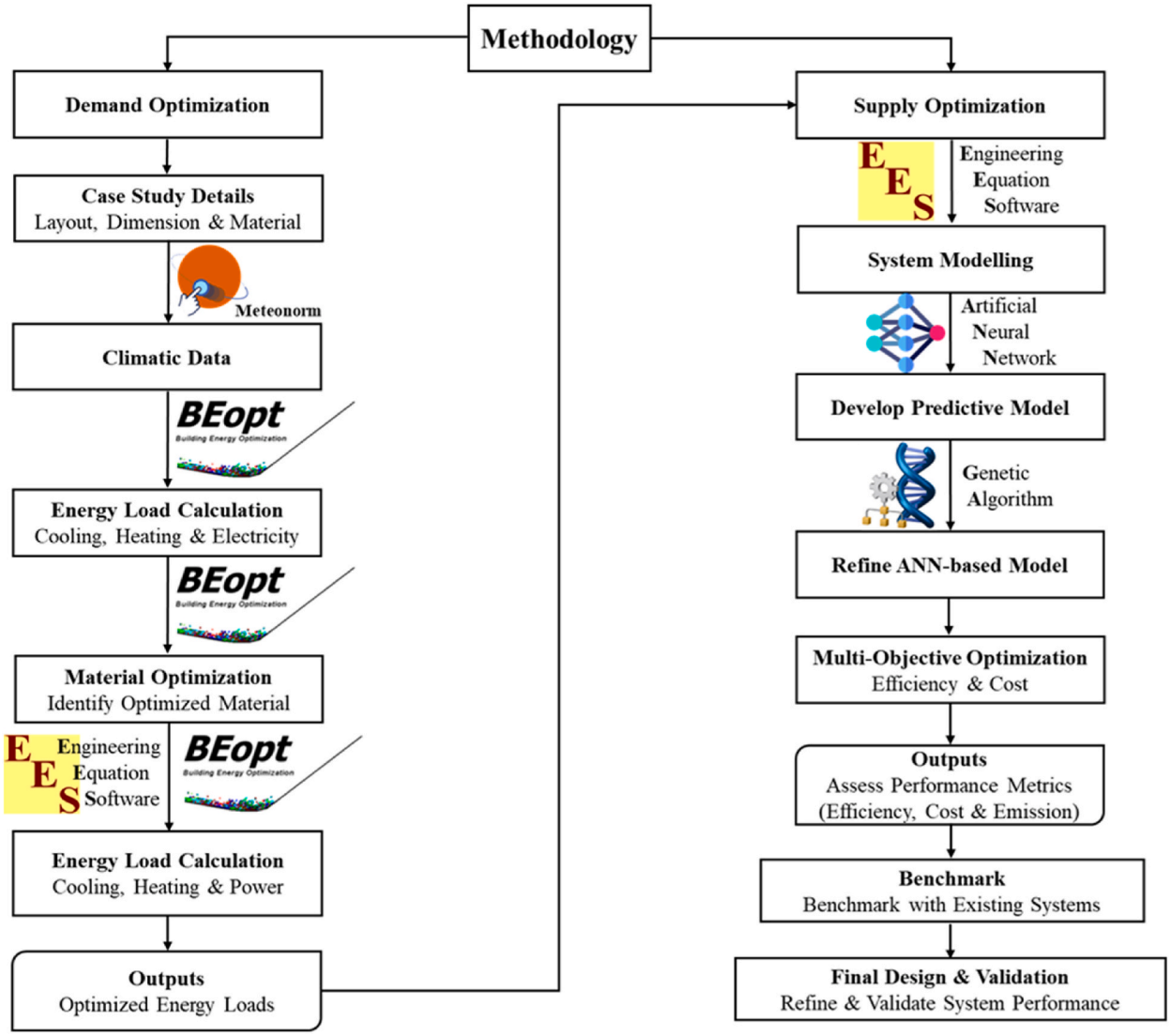

Fig. 1. Methodological framework.

2. **ANN Training and Prediction:** The simulation results from EES are used to train ANNs, which learn the complex relationships between design inputs and performance outputs (e.g., exergy efficiency and cost rate). Once trained, the ANN serves as a fast predictive model to evaluate new design scenarios.
3. **GA Optimization:** GAs use the ANN as a surrogate model to perform multi-objective optimization, searching for the optimal combination of system parameters that maximize exergy efficiency while minimizing cost.

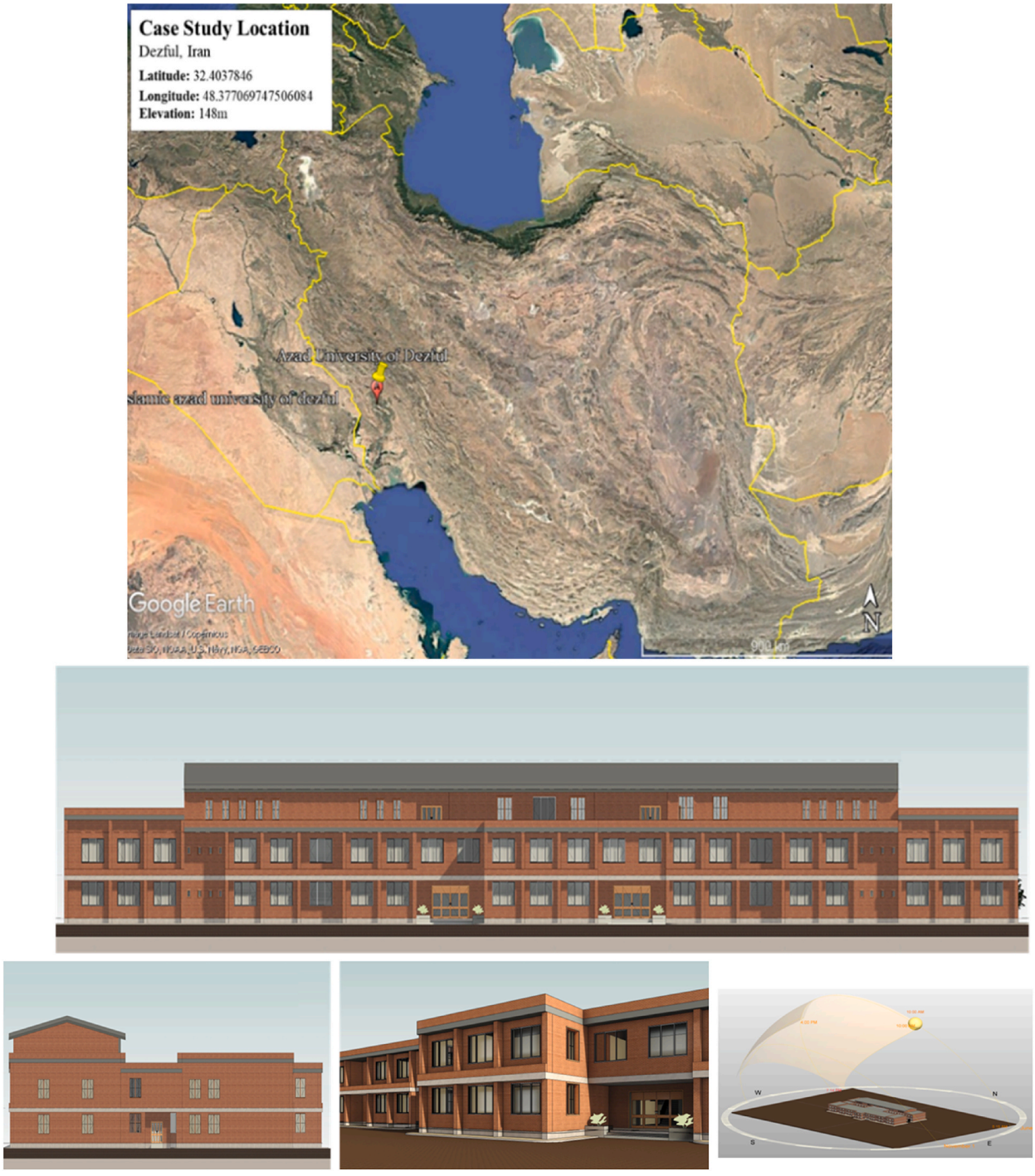

Fig. 2. Layout of the case study building.

Fig. 2. (*continued*).

4. **Validation and Final Evaluation:** The final design selected by the GA is validated by running a high-fidelity simulation in EES to confirm that the predicted performance metrics are held under thermodynamic principles. This ensures the optimized design is both practically viable and thermodynamically consistent.

This framework ensures the system meets refined loads efficiently and cost-effectively, supporting practical deployment for the case study building and climate.

2.3. Whole methodology

This study develops a holistic, scalable, and data-driven framework for optimizing multi-generation renewable energy systems in university campuses and large-scale settings, ensuring sustainability, energy efficiency, and cost-effectiveness. Demand-side optimization is achieved using BEopt and EES, incorporating Meteonorm climate data to optimize building materials and energy loads, thereby reducing cooling, heating, and electricity demand. On the supply side, a solar-powered multi-generation system is modeled using EES, with ANNs developing predictive models and GAs refining system parameters to enhance overall performance and operational stability. Finally, the optimized system is benchmarked against previous designs, with performance improvements assessed based on exergy efficiency, cost-effectiveness, and emissions reduction, ensuring a robust and validated approach to achieving ZEB goals.

Fig. 1 shows how this methodology brings together energy modeling, AI-based optimization, and thermodynamic analysis to connect demand-side efficiency with renewable energy supply, offering a comprehensive solution tailored for university energy systems.

3. Solar-powered multi-generation system design and optimization

This section is divided into two parts. Section 3.1 presents the case study, detailing its layout, dimensions, and material specifications. It also includes an analysis of climatic data and weather parameters, which are integrated into the BEopt software to determine the optimal building materials. This section also evaluates the cooling, heating, and electricity demand of the optimized building. Section 3.2 focuses on supply-side optimization, where a solar-powered multi-generation system is modeled using EES. ANN and GA are applied to refine system performance, ensuring optimal energy efficiency and cost-effectiveness.

3.1. Case study and energy demand analysis

In this study, the Engineering and Technology Building at the Islamic Azad University of Dezful (IAUD) is selected as the case study due to its high energy demand, extreme climatic conditions, and potential for optimization. The building comprises three floors with a total conditioned area of approximately 7270 m^2, as illustrated in Fig. 2. Located in Dezful City with extremely hot summers and mild winters (BSh, Köppen classification), the building is exposed to extreme thermal conditions, with maximum hourly temperatures reaching 55.6 °C in July and minimums dropping to 5.3 °C in January, making energy efficiency a critical design and operational concern. Its diverse functional spaces, including classrooms, laboratories, and offices, require continuous cooling, heating, and electricity, presenting an opportunity for energy performance enhancement. Fig. 2 shows the building's location, external views, and three-floor model and layout, including classes and offices.

As mentioned earlier, BEopt is a cost-effective tool for optimizing whole-building energy performance by modeling key parameters such as dimensions, design, occupancy, and location. It balances computational efficiency with practical insights, making it ideal for early-stage energy assessments and demand-side management. Table 1 presents essential details about the dimensions of the case study, based on the actual structure. These specifications provide a foundation for designing a replacement building that aligns with the existing faculty's size and layout.

Fig. 3 presents the energy optimization flowchart for the case study, outlining the process of calculating energy loads, optimizing material selection, and improving efficiency. This approach aims to reduce energy consumption and minimize environmental impact while supporting the design of a sustainable replacement for the existing faculty building.

Fig. 4 presents the monthly variations in key climatic parameters for Dezful, Iran, obtained from Meteonorm, highlighting their impact on the performance of the solar multi-generation system. The ambient temperature follows a distinct seasonal pattern, peaking at 39.6 °C in July and dropping to 11.3 °C in January, with prolonged high temperatures from April to September, increasing cooling demand. The dew point, representing moisture in the air, remains relatively stable but peaks at 12.8 °C in August, influencing latent cooling loads. Relative humidity decreases from winter (72.38 % in January) to summer (20.3 % in June), correlating with increased air dryness, which impacts evaporative cooling efficiency. Wind speeds fluctuate throughout the year, reaching 3.55 m/s in June, indicating a potential for integrating wind-assisted cooling strategies alongside solar energy. Higher wind speeds during summer contribute to faster moisture evaporation, further reducing relative humidity. Solar radiation, a critical driver of energy generation, exhibits a maximum Global Horizontal Irradiation (GHI) of 293.01 W/m^2 in June and a minimum of 108.08 W/m^2 in December, following the temperature trend. Diffuse irradiation, crucial for PV efficiency under cloudy conditions, remains moderate throughout the year, peaking at 231 W/m^2 in September. The interaction between these parameters significantly affects the system's efficiency; high GHI in summer enhances power generation but increases cooling demand, while lower winter irradiation necessitates optimized energy storage. Wind and humidity variations further influence system performance, particularly in balancing heating and cooling loads. This climatic analysis highlights the necessity of advanced optimization approaches to dynamically adjust system operations for efficiency and sustainability.

To design the proposed case study for optimal energy efficiency, various material types were evaluated using BEopt, considering their impact on energy demand reduction. Table 2 details the most effective features and materials identified through this process, ensuring a well-balanced combination of durability, sustainability, and energy-saving potential.

Fig. 5 illustrates the total monthly comparison of energy demand between the base case study and the optimized case study building. The optimized case study demonstrates clear energy performance improvements, particularly in cooling and total electricity use. Peak cooling demand in July was reduced from 2238.86 MWh in the base case to 1891.19 MWh in the optimized model, a 15.5 % reduction. In December, cooling demand dropped from 1077.08 MWh to 860.70 MWh, marking a 20.1 % improvement. Similarly, total electricity consumption declined across all months, with the July peak falling from 1371.44 MWh to 1169.70 MWh (a 14.7 % reduction), and the November low decreasing from 275.25 MWh to 213.03 MWh.

Table 1
Dimensions of the case study building.

Information	Unit	Value
Ground and First Floor Length	m	110
Ground and First Floor Width	m	51
Ground and First Floor Infrastructure	m^2	5670
Length of Second Floor	m	80
Width of Second Floor	m	20
Second Floor infrastructure	m^2	1600
Number of Floors	–	3

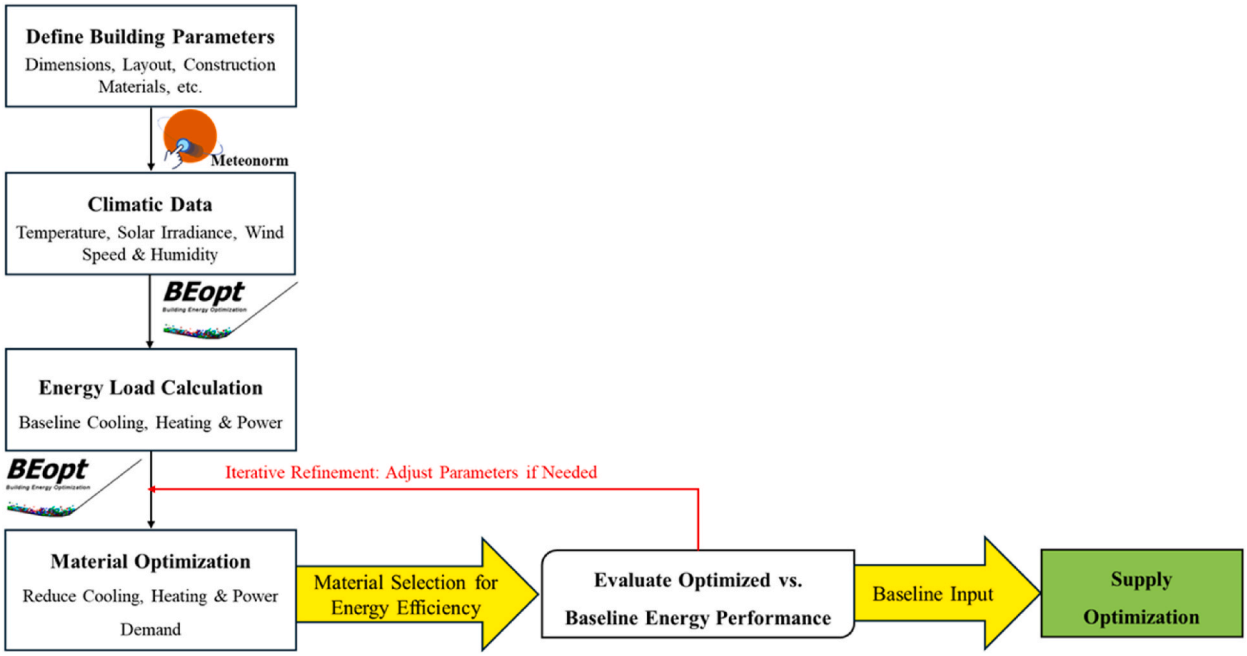

Fig. 3. Methodological flowchart for energy load calculation and optimization of the case study.

Lighting energy demand also benefited from the optimization, particularly during periods of high daylight availability. In January, lighting demand was reduced from 582.16 MWh to 582.17 MWh (almost unchanged), but notable reductions occurred in mid-year months, dropping from 259.65 MWh to 184.91 MWh in May, and from 290.50 MWh to 291.63 MWh in July. These savings are influenced by improved daylight access and interior reflectivity from optimized material selection. Seasonal changes play a major role in shaping all energy demands, with hot summers driving high cooling needs and longer daylight hours contributing to reduced lighting use. Overall, the optimized model improves energy efficiency and comfort, underscoring the importance of climate-responsive design.

Fig. 6 illustrates the thermal contours of energy consumption, showing hourly and monthly variations across cooling, heating, lighting, and total electricity demand. Cooling demand exhibits the highest intensity from June to August, peaking at over 120,000 kWh (red zones) during the day between 10:00 a.m. and 6:00 p.m., aligning with extreme summer temperatures in Dezful. Conversely, heating demand remains negligible throughout the year, with sporadic usage in January and December, reaching a maximum of 3800 kWh in the early morning hours (light blue zones). Lighting energy usage follows a distinct pattern, with peaks between 6:00 a.m.–8:00 a.m. (before working hours) and 6:00 p.m.–10:00 p.m. (after work hours), exceeding 74,000 kWh in winter months (yellow-red zones), indicating greater reliance on artificial lighting due to reduced daylight. Total electricity demand mirrors cooling trends, with peak usage exceeding 160,000 kWh in July and August, predominantly during daytime hours, as indicated by deep red regions. The transition from blue to red in the cooling and electricity contours highlights seasonal load shifts, emphasizing the importance of optimized building design and energy-efficient strategies to reduce peak demand, minimize operational costs, and maintain indoor comfort.

Table 3 summarizes the annual energy consumption of the optimized case study building, presenting the distribution of energy usage across cooling, heating, lighting, and total electricity demand. Cooling demand represents the largest energy component at 6326.109 MWh, making up approximately 41.4 % of the total electricity usage, reflecting Dezful's extreme summer temperatures. In contrast, heating accounts for the smallest energy consumption, representing just 0.04 % of total demand, confirming the minimal need for space heating due to the region's mild winters. Lighting energy usage accounts for 32.84 % of total consumption, emphasizing the need for efficient lighting systems, particularly during the winter months when artificial lighting is used more extensively. The total electricity demand shows the importance of integrating energy-efficient solutions across all end-uses, reinforcing the need for optimized cooling strategies, improved passive design techniques, and advanced lighting controls to reduce peak loads and enhance overall energy efficiency in university campus operations.

Table 4 presents a comparative analysis of energy costs, usage, and CO_2 emissions for the base and optimized building models, highlighting both economic and environmental outcomes. While the optimized building shows a slightly higher Life Cycle Cost (LCC) of $239,571.30 compared to $224,315 for the base case, it achieves a reduction in annualized energy costs from $6478 to $6162.48 and yields a favorable Net Present Value (NPV) of -$15,275.52 over its lifespan. Energy performance improvements include a 1.26 % reduction in annual energy consumption, 0.93 % savings in source energy, and a 0.91 % reduction in CO_2 emissions, decreasing from 37.18 to 35.34 metric tons/year. Although these improvements are modest, they validate the effectiveness of the proposed strategy and suggest that further enhancements, such as demand-side management, energy storage, or additional renewable integration, could

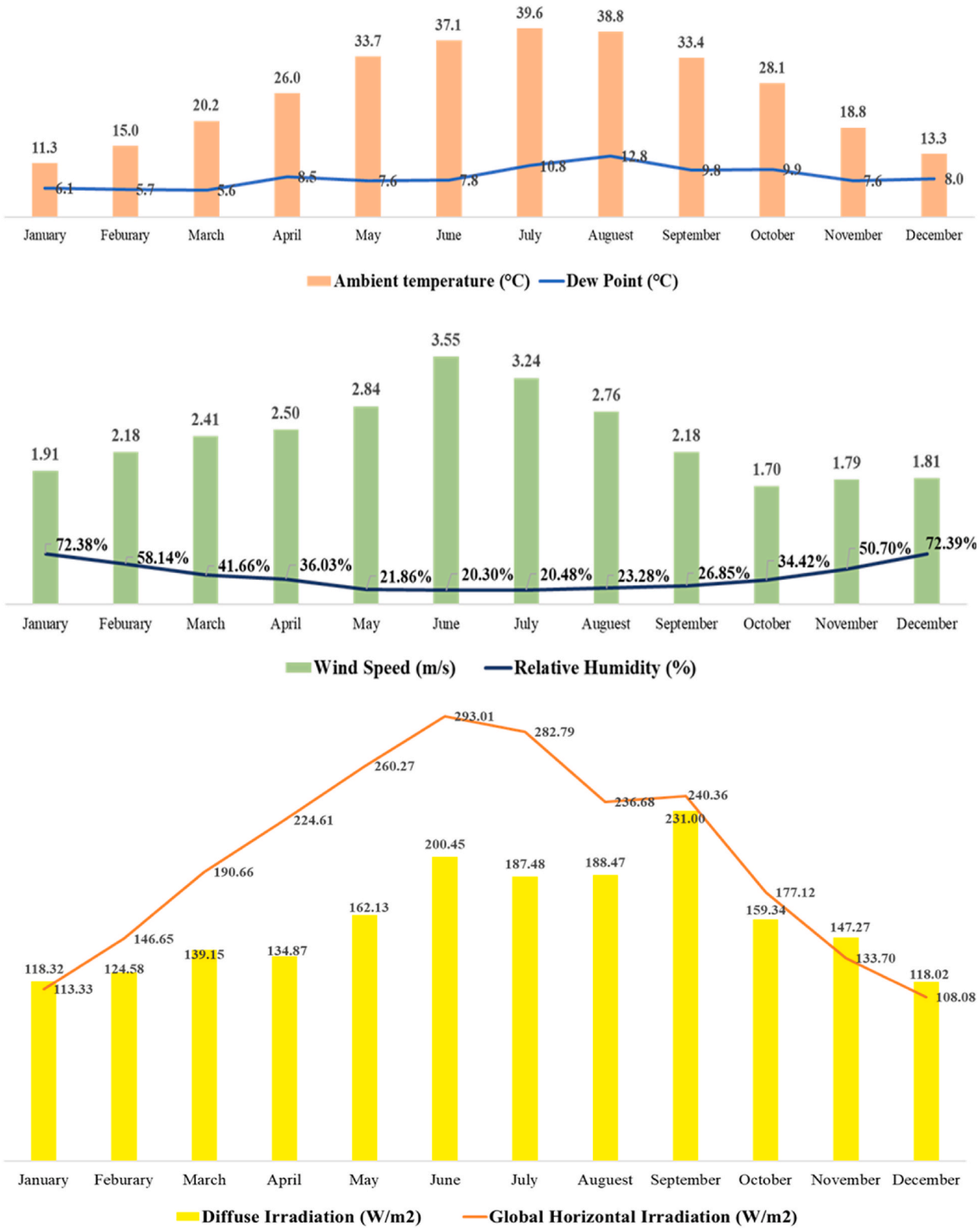

Fig. 4. Monthly variations in weather factors in dezful.

Table 2
Optimal building materials for energy efficiency.

Element	Optimal Material	Unit	Value
Windows	Back Windows = High-SHGC	–	–
Window Areas	–	in^2	20
Door	Fiberglass	–	–
Door Areas	–	in^2	1440
Wall Sheathing	OSB, R-15*PS	–	–
Exterior Finish	Aluminum, Light	–	–
Interzonal Walls	R-13 Fiberglass Batt	in	16
Wood Stud	Uninsulated	in	24
Double Wood Stud	R-45 Fiberglass, Gr-1, Centered	in	24
Steel Stud	R-19 Fiberglass Batt	in	24
Interior Shading	Summer = 0.7, winter = 0.7	–	–
Eaves	–	in	24
Overhangs	First Story, All Windows	in	24
Floor Mass	Gypsum Concrete	in	2
Exterior Wall Mass	PCM Drywall	–	–
Partition Wall Mass	Drywall	in	2*5.8
Ceiling Mass	PCM Drywall	–	–
Carpet	Carpet	%	40
Finished Roof	R-47.5 SIPs	–	–
Roof Material	Metal, Light	–	–
Lighting	LED	%	60
Pier & Beam	Ceiling R-19 Fiberglass Batt	–	–

amplify the benefits. These insights underscore the need for continued optimization to maximize long-term cost-effectiveness and decarbonization, setting the stage for the next section, which introduces the multi-generation solar energy system and its role in advancing sustainability.

3.2. Solar multi-generation system optimization

The multi-generation system used in this study is central to achieving the dual objectives of exergy efficiency and cost for the case study building. By simultaneously generating cooling, heating, lighting, and electricity, the system effectively meets diverse energy demands while reducing reliance on external energy sources. This section provides a detailed evaluation of the system's design, components, and integration with the optimized building structure, emphasizing its energy generation capacities, operational efficiencies, and flexibility to seasonal variations in energy consumption.

Fig. 7 illustrates the schematic of the proposed solar-powered multi-generation system, which integrates PV panels, a compressor, a condenser, an evaporator, and a thermal valve to optimize energy distribution. The solar farm harnesses renewable energy through an array of PV panels, generating electricity to power the compression-based cooling system while also supporting heating demands. The generated electricity drives the compressor, which circulates the working fluid through the system. The condenser extracts and delivers thermal energy for heating applications, while the evaporator provides cooling to the building. A thermal expansion valve regulates refrigerant flow, ensuring optimal thermal efficiency. This integrated system effectively balances heating and cooling loads, reducing dependence on grid-supplied electricity and enhancing the building's energy resilience. The strategic use of solar energy in this multi-generation configuration ensures efficient energy utilization, lowering operational costs and minimizing the carbon footprint of the university campus.

Artificial Intelligence Neural Networks (ANNs) consist of interconnected artificial neurons that process information similarly to biological neurons, enabling them to recognize complex data patterns and optimize learning processes [76,77]. Fig. 8 illustrates the ANN methodology used in this study, integrating a structured training flowchart with a schematic representation of the network's architecture. The figure presents a step-by-step training process for a feedforward, backpropagation ANN, beginning with input initialization, data formatting, and dataset division into training, testing, and validation subsets. The network iteratively trains by adjusting weights and biases while minimizing total error, validated against a final target threshold, if the error remains above this threshold, training continues; otherwise, the network proceeds to simulation. This figure also depicts the neural network structure, comprising input, hidden, and output layers, where neurons in the hidden layer apply weighted sums (W) and biases (B) to incoming signals before passing them through an activation function. This structure enables the ANN to capture non-linear relationships in energy consumption and optimization variables, ensuring accurate performance predictions and informed decision-making in the proposed system.

This study evaluated the solar farm thermally by applying mass and energy calculations to each control volume. To streamline the analysis while ensuring meaningful results, the following assumptions were made:

- Steady-state conditions are assumed, eliminating transient effects.
- Uniform water flow is considered throughout the pipes, ensuring consistent thermal exchange.
- No dust accumulation is assumed on the PV panels to prevent efficiency reductions.

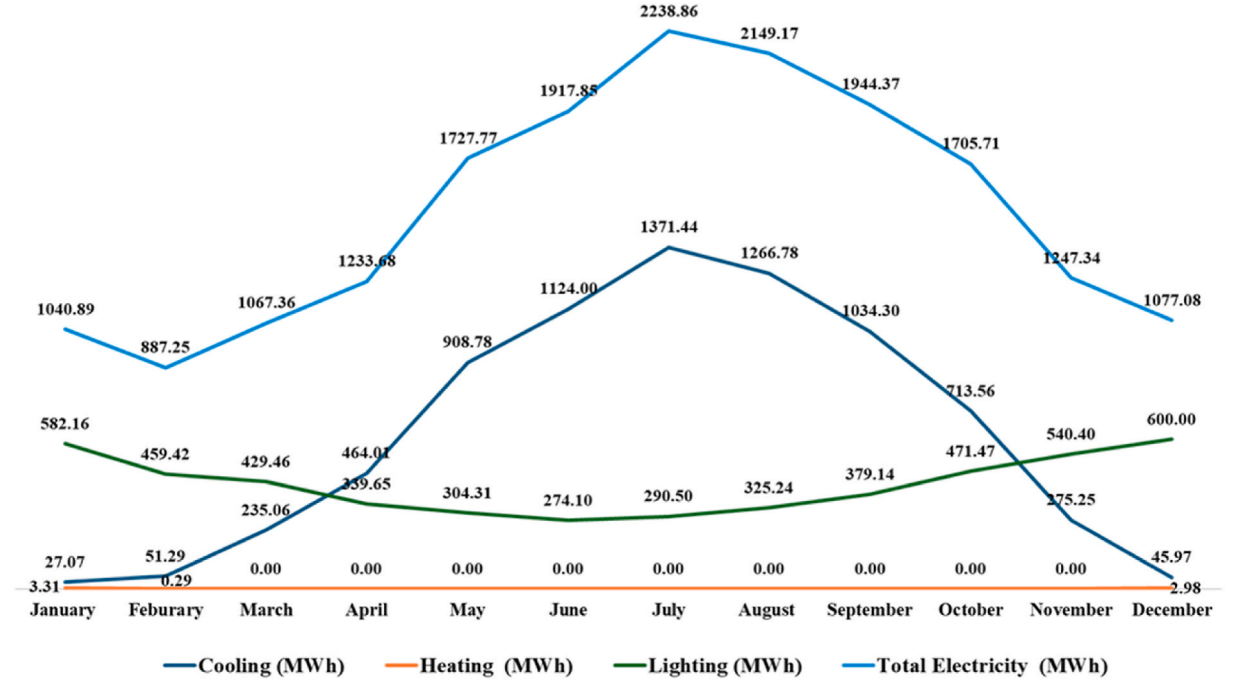

(b)

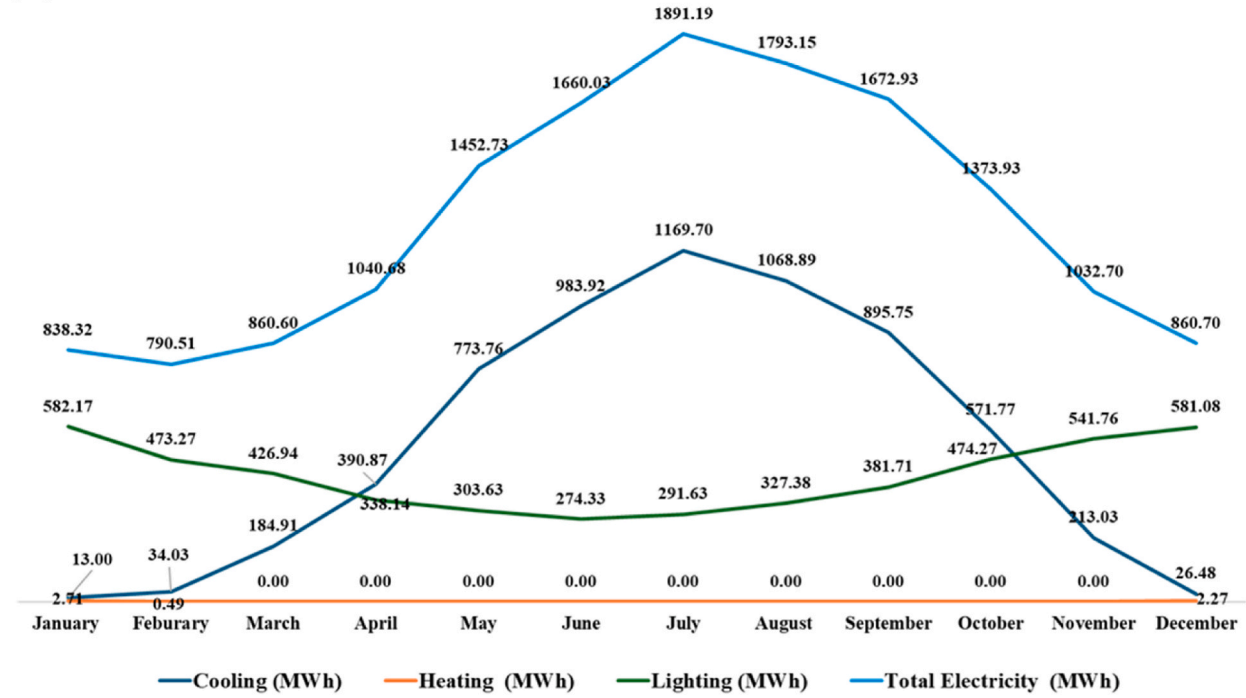

Fig. 5. Total monthly energy demand of the base case (a) and optimized case (b).

- Negligible side heat losses are considered, focusing energy calculations on primary thermal exchanges.
- Constant convective heat transfer coefficients are applied externally and internally along the panel surfaces to simplify the heat transfer model.
- Radiation exchange at the back of the panels is excluded, as its impact is relatively small compared to direct solar irradiation.
- Energy transfer is modeled as quasi-steady-state, allowing the use of simplified thermodynamic equations while maintaining accuracy.

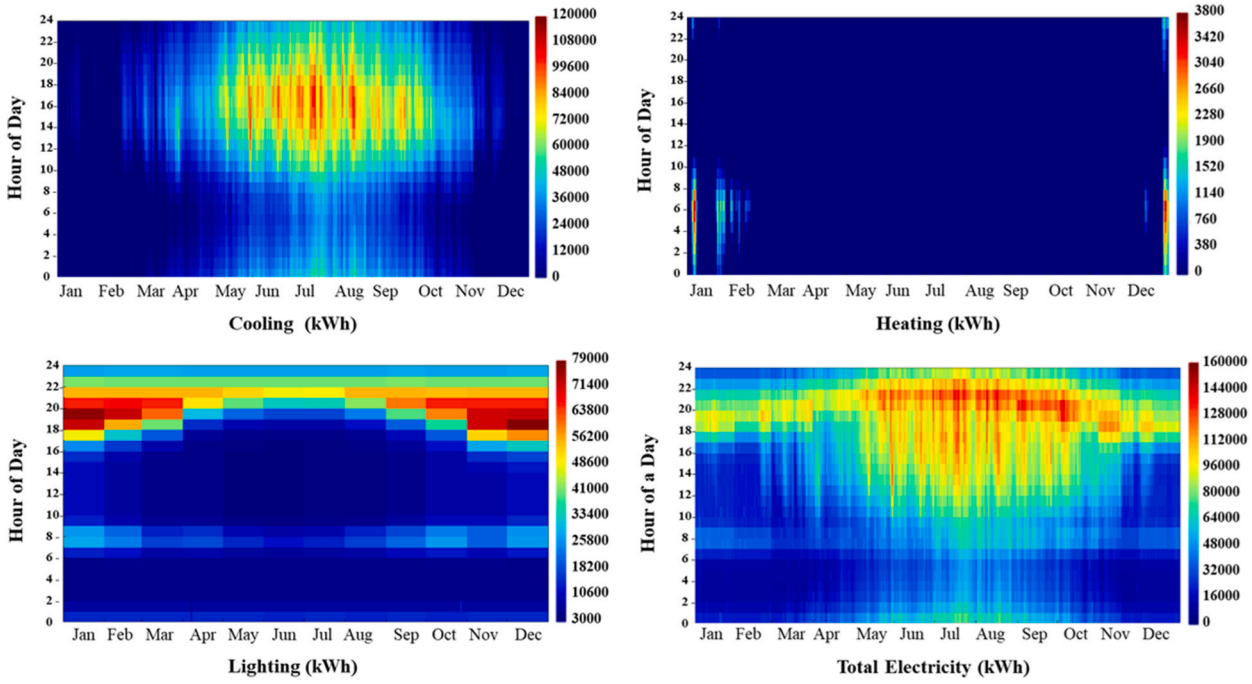

Fig. 6. Thermal contour map showing annual energy distribution for the optimized case study.

Table 3
Total annual energy usage of the optimized case study building.

Energy Usage	Unit	Value
Cooling	MWh	6326.109
Heating	MWh	5.462
Lights	MWh	4996.305
Total Electricity	MWh	15,267.484

Table 4
Energy costs, consumption, and CO_2 emissions for base and optimized building.

Parameter	Unit	Base Case	Optimized Case
LCC	$	224,315	239,571.3
Annualized Energy Costs	$/yr	6478	6162.48
Annual Energy Savings	%/yr	–	1.26
CO_2 Emissions	Metric tons/yr	37.18	35.34
Annual Source Energy Savings	%/yr	–	0.93
NPV of Energy-Related Costs	$	–	−15,275.52
AnnualCO_2 Savings	%/yr	–	0.91

These assumptions reduce computational complexity while ensuring precise performance evaluation. The fundamental equations for this analysis are available in the relevant literature [62,78]. The key input parameters used in the thermodynamic analysis of the solar farm are summarized in Table 5.

The thermodynamic analysis follows fundamental energy balance principles to evaluate the solar farm's performance. Equation (1) demonstrates how the first law of thermodynamics is applied to each control volume and provides the basis for analyzing energy interactions within the proposed solar PV-thermal system.

$$\dot{Q} - \dot{W} + \sum_i \dot{m}_i \times \left(h_i + \frac{v_i^2}{2} + gZ_i\right) - \sum_e \dot{m}_e \times \left(h_e + \frac{v_e^2}{2} + gZ_e\right) = \frac{dE_{Cv}}{dt} \tag{1}$$

Here, $\dot{Q}$ is the heat transfer rate into the control volume? $\dot{W}$ is the work done by the system, $\dot{m}_i$ and $\dot{m}_e$ are mass flow rates at the inlets and outlets, h is the specific enthalpy, v is velocity, g is gravitational acceleration, Z is elevation, and E_{Cv} is the total energy within the control volume. This foundational equation. The measure of useful energy generated by the solar PV panels is calculated using

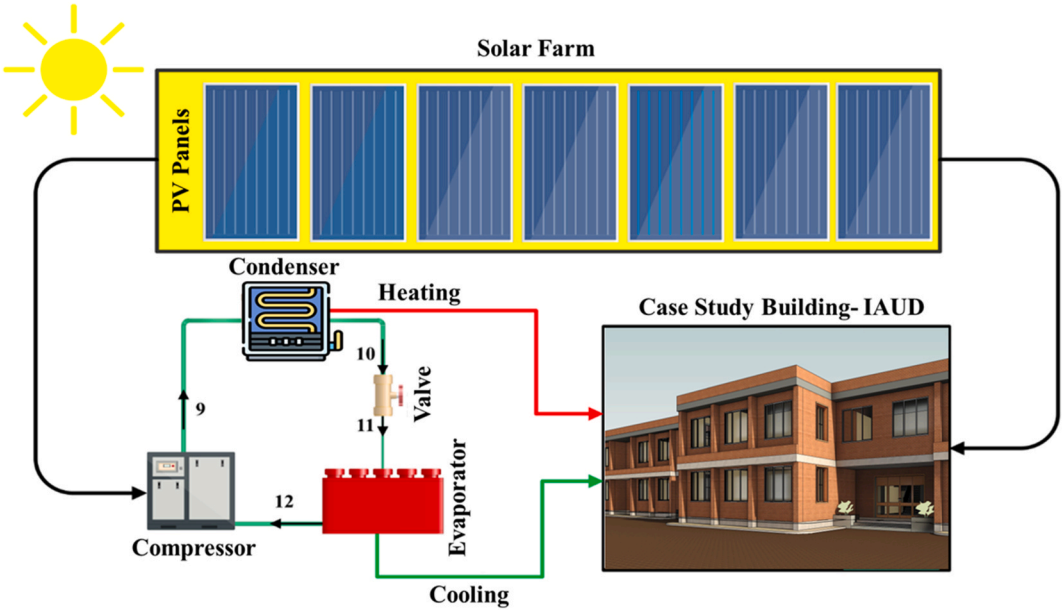

Fig. 7. Schematic of the proposed solar farm.

Equation (2):

$$\dot{Q}_{PV} = \frac{\dot{m}_{air} \times C_{air}}{U_l} \times \left(h_{p2g} \times Z \times GB\right) - U_l \times \left(T_{air,in} - T_0\right) \times \left(1 - \frac{\exp(-b \times U_l \times L)}{\dot{m}_{air} \times C_{air}}\right) \tag{2}$$

Equation (2) estimates the amount of heat transferred from the PV panel to the surrounding air, considering the air mass flow rate, specific heat capacity, solar irradiance, and system geometry. In this equation, $\dot{Q}_{PV}$ is the useful thermal energy output (kW), $\dot{m}_{air}$ is the air mass flow rate (kg/s), C_{air} is the specific heat of air (kJ/kg.K), U_l is the overall heat transfer coefficient (W/m^2.K), h_{p2g} is the secondary heat transfer coefficient, GB is the beam solar radiation (W/m^2), $T_{air,in}$ is the inlet air temperature (°C), T_0 is the ambient temperature (°C), b is a collector width parameter (m^{-1}), and L is the panel length (m).

The electrical power output generated by PV panels is determined using Equation (3).

$$W_{PV} = \frac{\eta_C \times GB \times B_C \times tau_g \times A}{10} \tag{3}$$

Equation (3) provides a direct estimate of the electricity produced under given solar conditions. W_{PV} is the electrical power generated by the PV system (kW), η_C is the PV module's conversion efficiency, tau_g is the transmissivity of the glass cover, and A ($b \times L$) is the surface area of the collector (m^2).

Equation (4) calculates thermal efficiency, which represents the proportion of incoming solar energy that is successfully converted into useful thermal energy. It serves as a key performance indicator for assessing the heat recovery capability of the PV system.

$$\eta_{th} = \frac{\dot{Q}_{PV}}{GB \times A} \tag{4}$$

In this equation, η_{th} is the thermal efficiency.

3.3. Empirical validation of PV simulation results

To ensure the reliability of the simulation results, validation was conducted by comparing the PV subsystem outputs from the present study with empirical data from a previously published study [79], which validated TRNSYS by estimating electricity yields from a fixed-slope 90 Wp PV panel installed in Cape Town, South Africa. Their model predictions, based on nearby weather station data, were closely aligned with actual measured yields, achieving kappa values of 0.722 and 0.944 at 90 % and 80 % acceptance ratios, respectively. The regression coefficient for modeled versus measured incident solar energy on a horizontal plane was 0.782, confirming the predictive strength of the simulation. In the current study, PV output data from 18 days showed strong agreement with the reference study findings [79], with most values differing by less than ±0.02 kWh, thereby validating the numerical accuracy of the current simulation framework for PV performance modeling.

Table 6 shows that the daily power differences remained within ±6.3 %, with most deviations falling below ±3 %. The consistency of this agreement highlights the robustness of the current simulation methodology in accurately predicting PV energy yields under

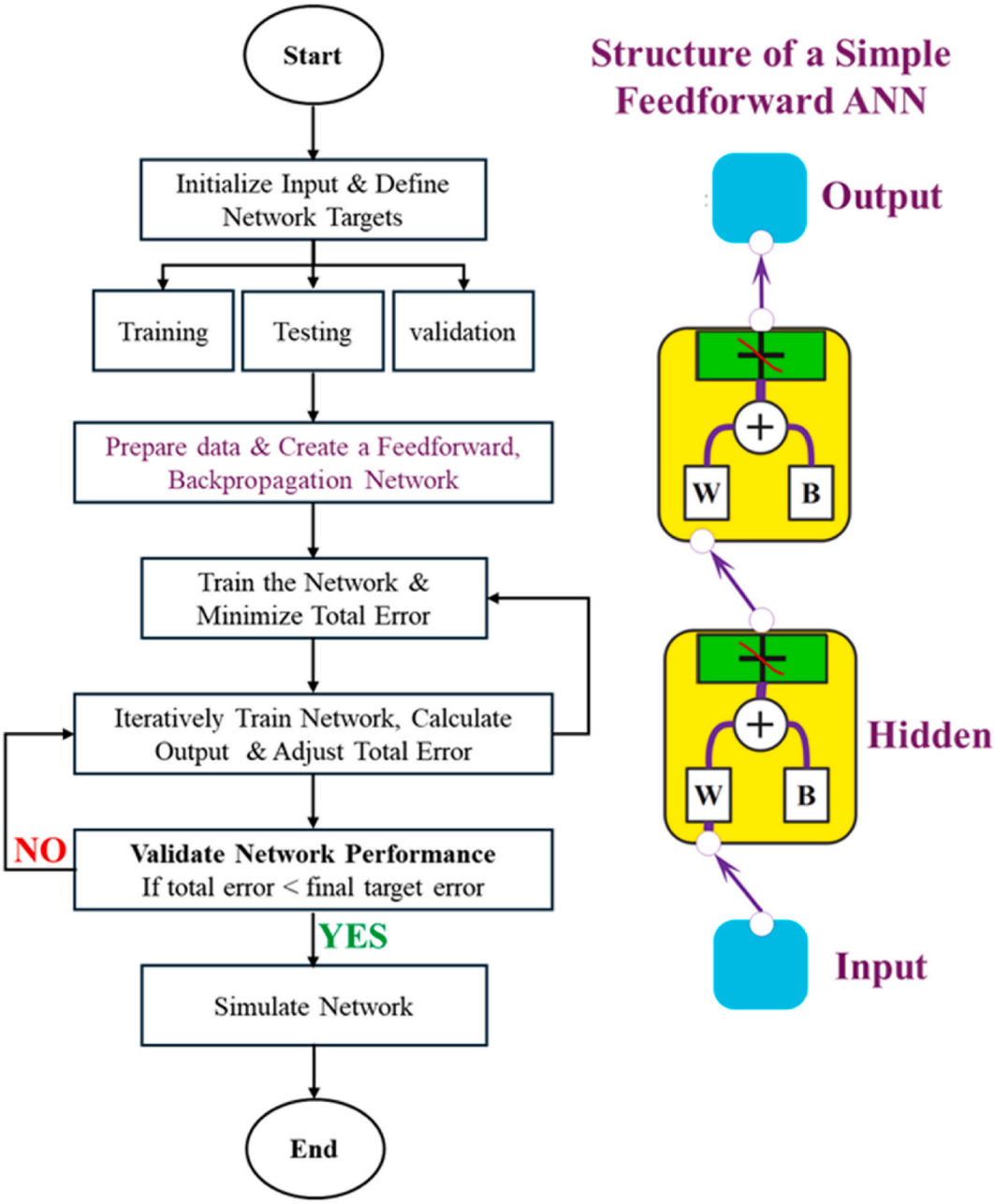

Fig. 8. Neural network training flowchart and architecture for energy optimization.

Table 5
Input data for solar farm analysis.

Parameter	Unit	Value
T_0	°C	25
P_0	kPa	101.3
n	–	80
T_{sun}	°C	6000
$\dot{m}_{air}$	kg/s	1.9
U_l	W/m^2 K	4.71
L	m	2.5
b	m	0.8
A	m^2	2

Table 6
Comparison of simulated PV outputs with validated TRNSYS data.

Day	PV Power (kWh)		Deviation (%)
	Present Paper	Referenced Study [79]	
1	0.5	0.5	0
2	0.73	0.74	−1.35
3	0.58	0.56	3.57
4	0.62	0.64	−3.13
5	0.56	0.53	5.66
6	0.63	0.66	−4.54
7	0.54	0.52	3.85
8	0.63	0.64	−1.56
9	0.61	0.6	1.67
10	0.7	0.74	−5.41
11	0.64	0.63	1.59
12	0.51	0.5	2.00
13	0.49	0.48	2.08
14	0.6	0.64	−6.25
15	0.7	0.68	2.94
16	0.65	0.66	−1.52
17	0.63	0.64	−1.56
18	0.58	0.56	3.57

real-world climatic conditions. This validation strengthens confidence in the proposed multi-generation system's design and confirms the applicability of the modeling framework to performance estimation and decision-making for renewable energy integration.

4. Results and discussion

The section presents the study's findings, emphasizing the impact of multi-objective optimization on enhancing energy performance within the case study. By integrating advanced optimization techniques, the study simultaneously evaluates multiple objectives, energy efficiency, cost reduction, and environmental impact. This holistic approach ensures a well-balanced energy strategy that meets the building's diverse operational demands while maximizing the potential of the proposed solar-powered multi-generation system. Section 4.1 provides a detailed analysis of the optimization outcomes, examining the influence of each optimized variable on system performance and overall sustainability.

4.1. Multi-objective optimization

This research utilized a combination of neural network methods and algorithms to optimize the solar farm's performance, aiming to enhance efficiency while reducing costs. The optimization parameters in Table 7 were carefully selected to balance energy generation, space constraints, and economic feasibility. The range for the number of panels ensures scalability while avoiding excessive installation costs. The panel dimensions were optimized to maximize solar capture without exceeding practical design limitations. The efficiency range reflects realistic advancements in PV technology, ensuring that the selected panels align with commercially viable options. By optimizing these variables, the study achieves an effective trade-off between performance, cost, and space utilization, enhancing the feasibility of the proposed system.

The goal of this optimization is to enhance system performance by improving technical parameters, such as exergy efficiency, while simultaneously minimizing costs. Table 8 presents the optimal values for the four decision variables used in the technical and economic optimization, along with the corresponding optimal values of the objective functions. The optimization results indicate that an optimal PV panel configuration consists of 120 panels with a width of 2 m^2, a length of 3.5 m^2, and an efficiency of 40 %, ensuring a well-balanced trade-off between energy generation and system feasibility. The objective function results demonstrate that the exergy efficiency was optimized to 23.45 %, within the range of 11.4 %–38.02 %, while the cost rate settled at $14.93/h, balancing affordability and efficiency. This optimization was conducted using 500 data points, extracted from the system modeling solution, which were processed through a neural network and refined using meta-heuristic algorithms. The large dataset improves the accuracy of the optimal solution, ensuring a robust balance between energy efficiency and economic feasibility.

Fig. 9 illustrates the variation range of the objective functions, exergy efficiency and cost rate, along with their optimal values. The

Table 7
Optimization parameters ranges.

Variable	Unit	Lower Bound	Upper Bound
PV Panel Number	–	80	160
PV Panel Width	m^2	0.5	3.5
PV Panel Length	m^2	2.5	4.5
PV Panel Efficiency	%	30	50

Table 8
Optimal amount for decision variables and objective functions.

Decision variables		Unit	Optimum Point		N
PV panel number (−)		–	120		500
PV panel width (m^2)		m^2	2		500
PV panel length (m^2)		m^2	3.5		500
PV panel efficiency (%)		%	0.4		500
Objective Functions	Unit	Valid N	Optimal Point	Minimum	Maximum
Exergy efficiency (%)	%	500	23.4465	11.4	38.02
Cost rate	$/h	500	14.92773	2.275	36.4

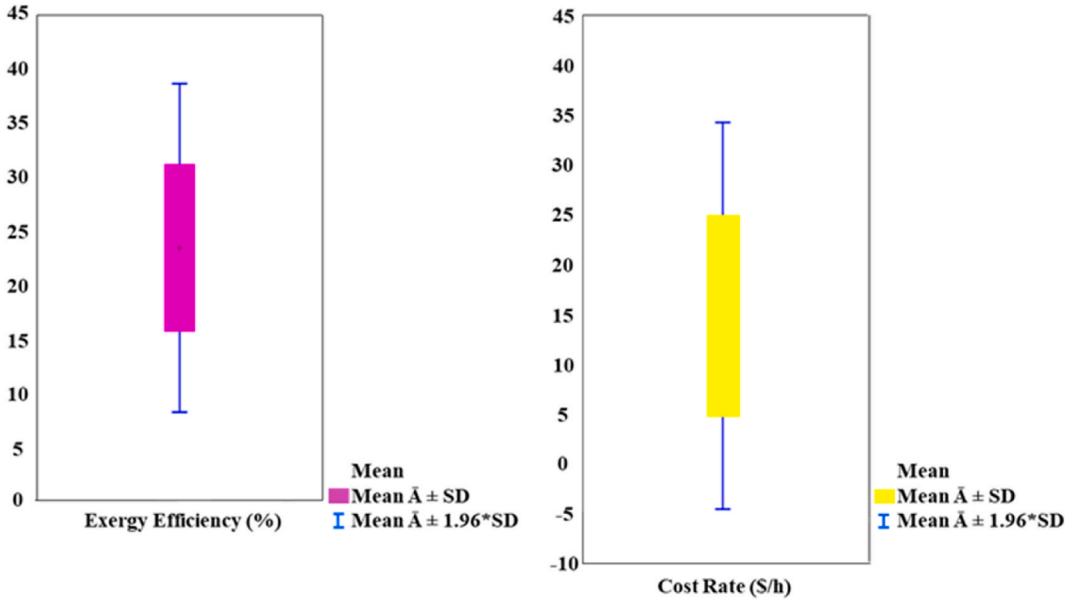

Fig. 9. Variation range of objective functions for the optimized multi-generation system.

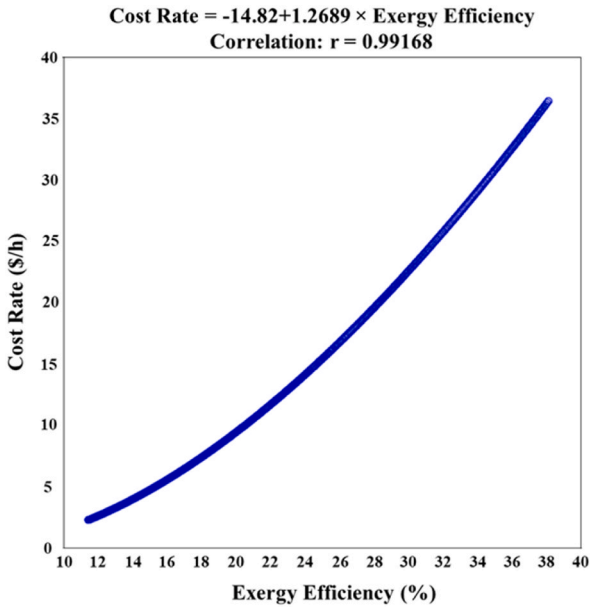

Fig. 10. Pareto chart: Trade-off between exergy efficiency and cost rate in the optimized case.

box plots show the distribution of values, where the Interquartile Range (IQR) highlights the spread of results, and the whiskers indicate the full range of variation. Exergy efficiency exhibits a broad range, spanning approximately 11.4 %–38.02 %, with an optimal value centered around 23.45 %, suggesting significant variability in system performance depending on the selected parameters. Similarly, the cost rate varies widely between $2.28/h and $36.4/h, with an optimal cost rate of $14.93/h, emphasizing the trade-off between economic feasibility and efficiency. The mean values for both objective functions fall well within their respective ranges, confirming the robustness of the optimization approach. These variations underscore the importance of multi-objective optimization in balancing technical and economic performance, ensuring that the system operates efficiently while maintaining cost-effectiveness.

Multi-objective optimization is employed to determine optimal trade-offs between conflicting objectives, ensuring a balanced solution that enhances system performance. Fig. 10 presents the Pareto chart illustrating the relationship between exergy efficiency and cost rate, with a clear positive correlation. The Pareto front demonstrates that as exergy efficiency increases, the cost rate rises exponentially, highlighting the trade-off between economic feasibility and technical performance. The fitted equation confirms this relationship, while the correlation coefficient ($r = 0.99168$) indicates a strong dependency between these two variables. This high correlation suggests that improving exergy efficiency inevitably leads to a higher cost rate, reinforcing the need for careful parameter selection to balance efficiency gains with affordability. The consistency of the Pareto front and the low variance in the solution set validate the robustness and accuracy of the optimization process, ensuring that the selected optimal solutions align with practical implementation constraints.

Fig. 11 presents histograms illustrating the distribution of exergy efficiency and cost rate, providing insights into the training and calculation processes. The cost rate histogram follows a slightly skewed distribution, with a higher frequency of observations around lower cost values, while the exergy efficiency histogram exhibits a more balanced distribution centered around moderate efficiency levels. Both distributions are overlaid with expected normal curves, showing how the data aligns with a standard distribution. The results indicate that while exergy efficiency values are relatively well-distributed, cost rate values show a wider variation, reflecting the inherent trade-off in the optimization process. These histograms validate the robustness of the dataset used in the optimization, ensuring a well-represented range of possible system performance outcomes.

Fig. 12 depicts the half-normal probability plots for the cost rate and exergy efficiency, illustrating their alignment with expected normal distributions. Both plots exhibit a nonlinear trend, particularly at the upper range, indicating slight deviations from perfect normality. The cost rate distribution shows a more pronounced deviation at higher values, suggesting greater variability in higher cost scenarios. Similarly, the exergy efficiency plot follows a comparable trend, with larger deviations observed at efficiency levels beyond 35 %. These deviations indicate that while the data follows an approximate normal distribution, some outliers or skewness may be present, particularly in the upper range. These findings highlight the importance of considering statistical variations in optimization processes to ensure robust and reliable results.

Fig. 13 compares the predicted and actual values for cost rate and exergy efficiency, demonstrating the accuracy of the trained predictive model. The optimization process utilized a combination of ANN and GA to enhance predictive accuracy. The regression equations for both objective functions show a strong linear correlation, with $r = 0.97957$ for cost rate and $r = 0.99731$ for exergy efficiency, indicating near-perfect predictive performance. The predicted values closely follow the actual data points, confirming the model's ability to generalize the relationship between optimization parameters and system performance. The high correlation values suggest that the applied ANN-GA-based optimization effectively captures the underlying trends, ensuring reliable predictions for cost and exergy efficiency under varying conditions. These results validate the robustness of the predictive model, supporting its application in optimizing the solar-powered system with high accuracy. The close match between predicted and actual values ($r = 0.97957$

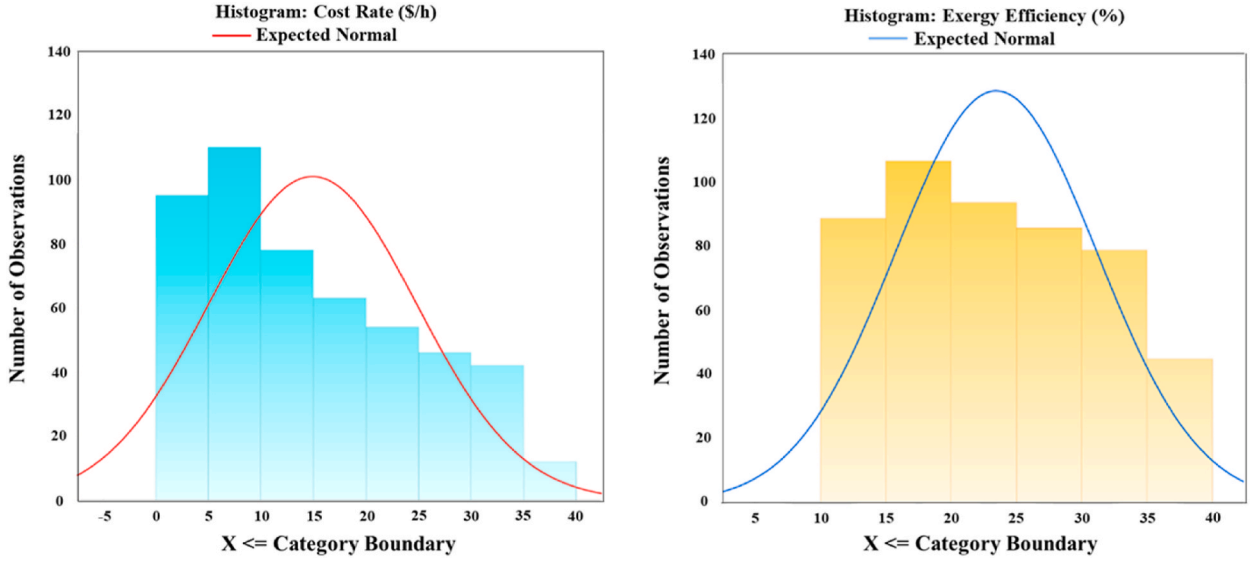

Fig. 11. Objective functions histogram for the optimized case with expected normal distributions.

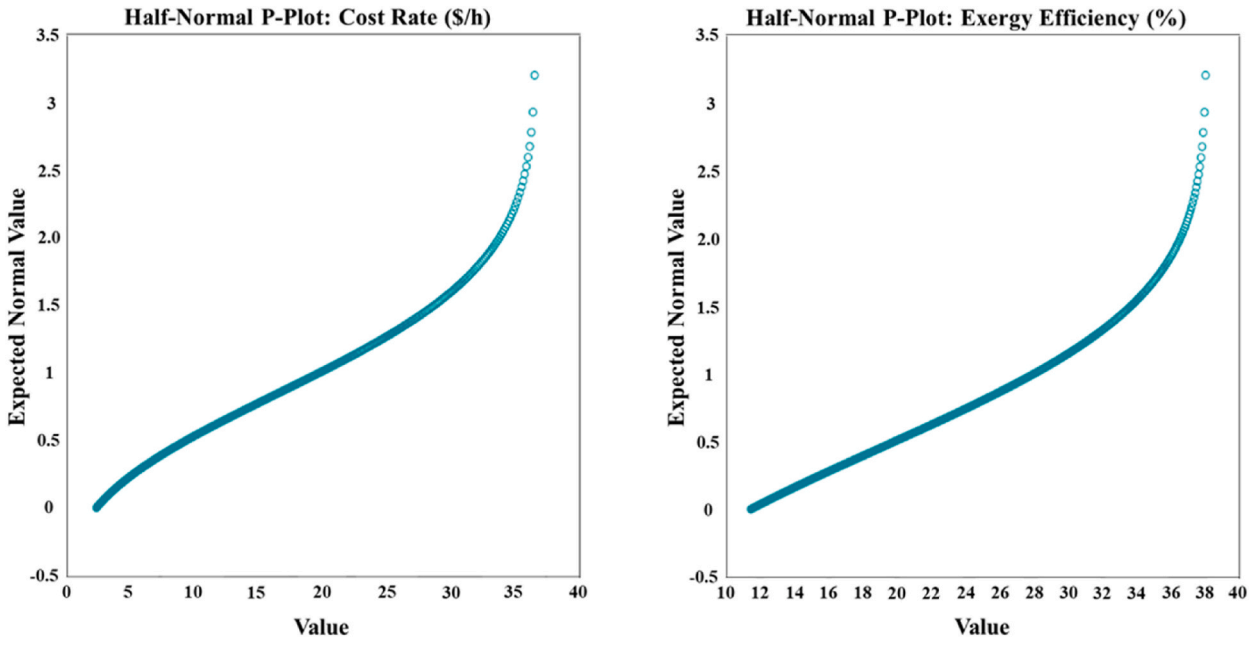

Fig. 12. Half-normal probability plots for cost rate and exergy efficiency in the optimized case.

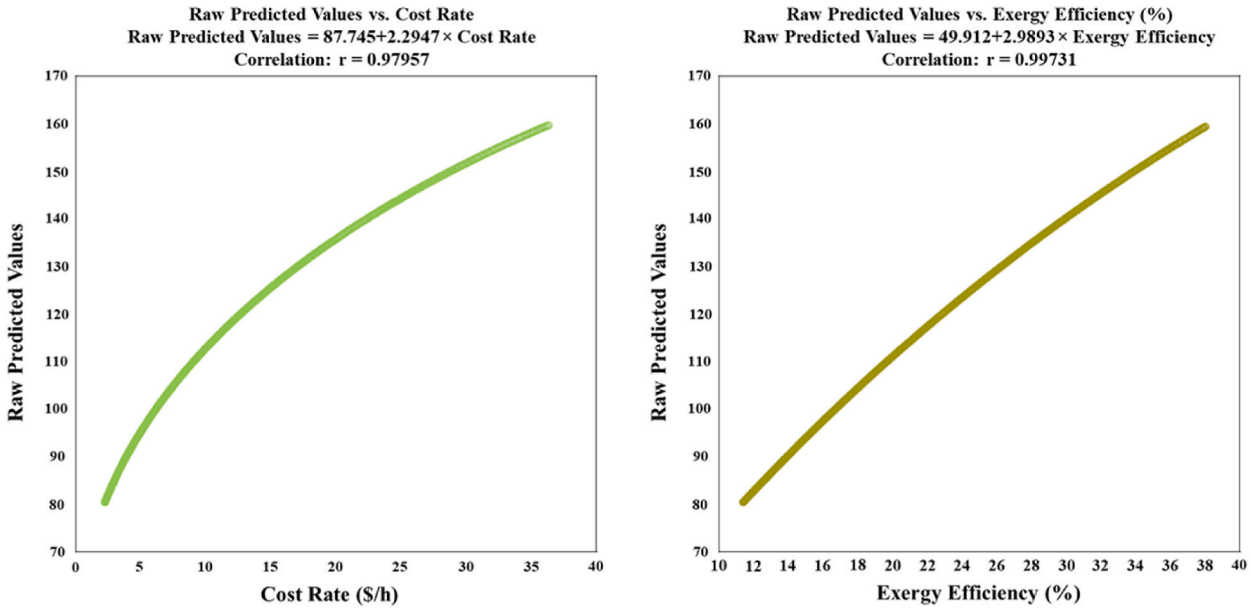

Fig. 13. Predicted vs. Actual Values of Objective Functions in the Optimized System.

for cost rate; r = 0.99731 for exergy efficiency) suggests that the ANN-GA optimization model is highly accurate and reliable.

Fig. 14 illustrates the normal probability distribution of residuals for exergy efficiency and cost rate, evaluating the goodness-of-fit of the predictive model. The normal P-plots indicate a generally S-shaped distribution, with minor deviations at the lower and upper tails. The residuals mostly align with the expected normal line, confirming a well-distributed error structure. However, slight deviations occur beyond the 95th percentile, where residuals tend to be slightly higher for exergy efficiency (>38 %) and cost rate (>35 $/h), indicating potential outliers in extreme cases. Despite these variations, the majority of residuals remain within ±2 standard deviations, ensuring that predictions are statistically reliable. The high correlation values (close to 1.0) further validate the ANN-GA model's predictive accuracy, reinforcing its robustness for optimizing system performance.

Fig. 15 indicates the detrended normal probability plots for cost rate and exergy efficiency, highlighting deviations from the expected normal distribution. The residuals fluctuate around zero, suggesting a generally well-distributed error structure; however,

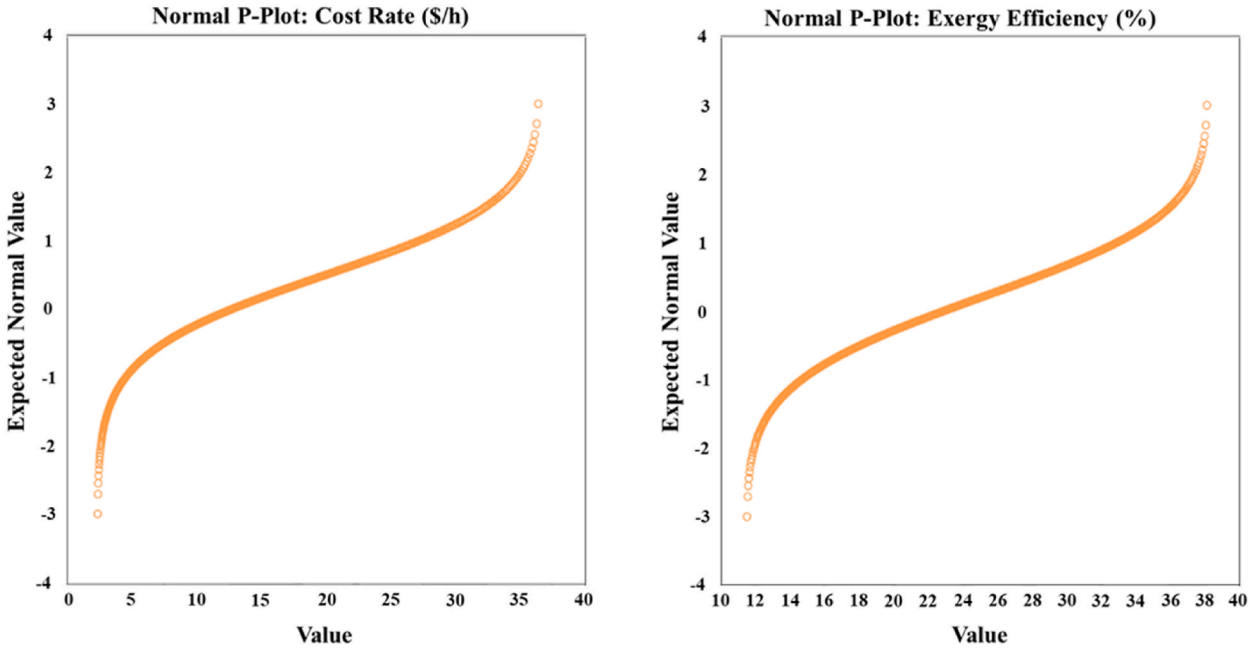

Fig. 14. Normal probability plots of residuals for optimized multi-generation system.

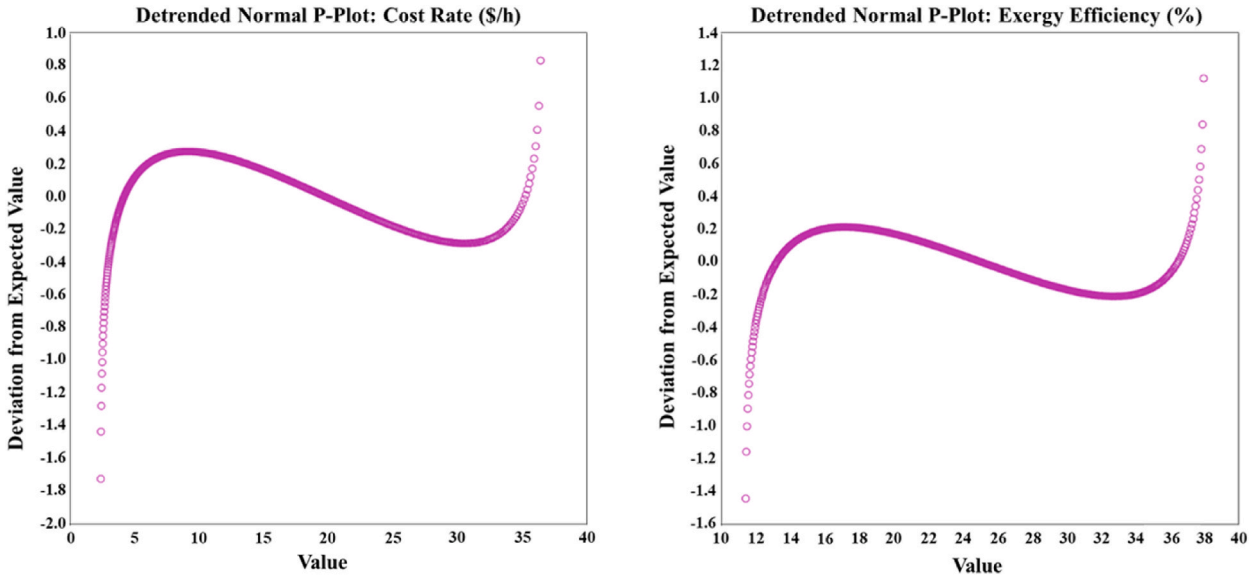

Fig. 15. Detrended normal probability plots for objective functions in the optimized case.

larger deviations are observed at both lower and upper extremes, particularly beyond 35 $/h for cost rate and 38 % for exergy efficiency. The residual spread at these extremes suggests the presence of minor nonlinearity or potential outliers influencing the predictions. Despite these variations, the majority of residuals remain within ±1.5 standard deviations, confirming that the predictive model effectively captures the general trend with only slight deviations at extreme values. These findings emphasize the robustness of ANN-GA optimization while identifying regions where further refinement may enhance predictive accuracy.

The multi-objective optimization conducted in this study effectively enhanced the solar farm's performance by achieving an optimal balance between efficiency and cost-effectiveness. The results highlight that optimizing PV panel parameters, including efficiency, dimensions, and the number of panels, significantly improves energy generation while ensuring economic feasibility. The AI-driven optimization approach successfully addressed the trade-offs between exergy efficiency and cost rate, ensuring that the final design met both technical performance and budgetary constraints. Statistical analyses, including Pareto front evaluation, probability

distribution analysis, and residual diagnostics, confirm the robustness and reliability of the optimization process. By minimizing deviations and aligning predictive models with observed data, the study validates the use of advanced optimization techniques for improving energy system performance. The findings emphasize the importance of integrating AI-driven optimization into solar-powered multi-generation systems, offering a practical, scalable, and sustainable solution for energy-efficient infrastructure in multi-functional environments.

4.2. Economic and environmental impact

This section indicates the economic and environmental impact of the optimal multi-generation system. Fig. 16 illustrates the total cost rate distribution for the proposed solar farm, breaking down the financial contribution of its key components: the solar array and the compression chiller unit. The analysis reveals that the solar array accounts for the dominant share of total costs, contributing 13.54 $/h, representing over 94 % of the total operational expenditure. Financial cost calculations were based on a fixed average electricity price of 0.15 USD/kWh. The reduction in energy costs was determined by multiplying the total annual electricity savings by this fixed tariff rate, without incorporating variable pricing schemes. Net-billing systems, which apply variable energy prices based on time-of-use or surplus electricity export rates, were not included in this analysis. This cost is directly linked to the installation and maintenance of 120 PV panels, optimized for energy generation efficiency. In contrast, the compression chiller unit incurs a notably lower cost of 0.892 $/h, contributing only 6 % to the total cost rate. The disproportionate cost distribution highlights the financial priority of PV optimization, as reducing panel-related expenses would have the most substantial impact on overall economic feasibility. These findings reinforce the need for strategic cost reduction in solar array deployment, ensuring that the system remains both energy-efficient and financially sustainable.

Fig. 17 illustrates the environmental benefits of the solar-powered multi-generation system, which significantly reduces CO_2 emissions and environmental costs while meeting the faculty's energy demands. The system generates a total net output of 49,545.39 MWh, offsetting emissions that would otherwise reach 10,113.38 tons of CO_2 annually, as conventional power plants emit 0.204 tons of CO_2 per MWh. This reduction translates into $242,721.1 in avoided environmental costs, based on a $24 per ton CO_2 rate. Additionally, the project supports green space expansion, providing an estimated 49 ha of environmental benefit. These results highlight the system's dual impact in lowering pollution and promoting sustainability, reinforcing the importance of renewable energy solutions in large-scale applications. It is important to note that the CO_2 emission analysis in this study focuses solely on operational emissions associated with heating, cooling, and electricity consumption. Emissions arising from the full life cycle of the building, including construction, material production, and end-of-life stages, were not included in this analysis.

4.3. Solar farm energy output, surplus utilization, and storage

The study examines the solar farm's heating and cooling outputs, which vary with weather conditions and are directly linked to the operation of a compression chiller powered by solar-generated electricity. Fig. 18 illustrates the total monthly cooling, heating, and

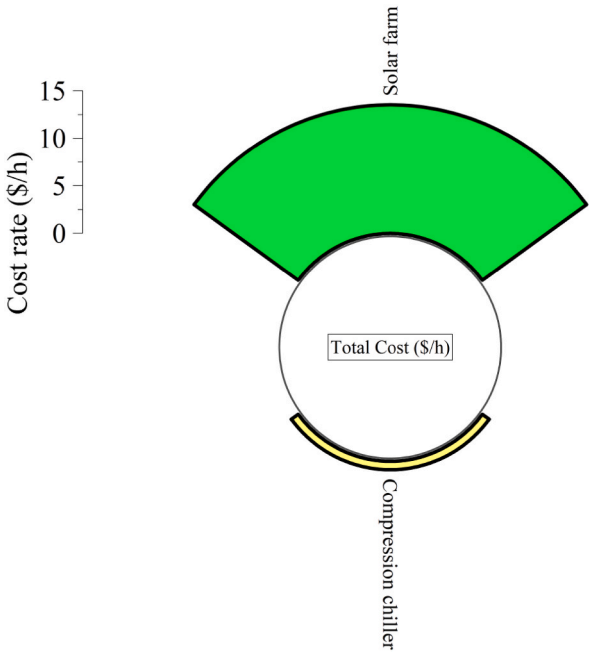

Fig. 16. Cost rate of optimized solar farm components.

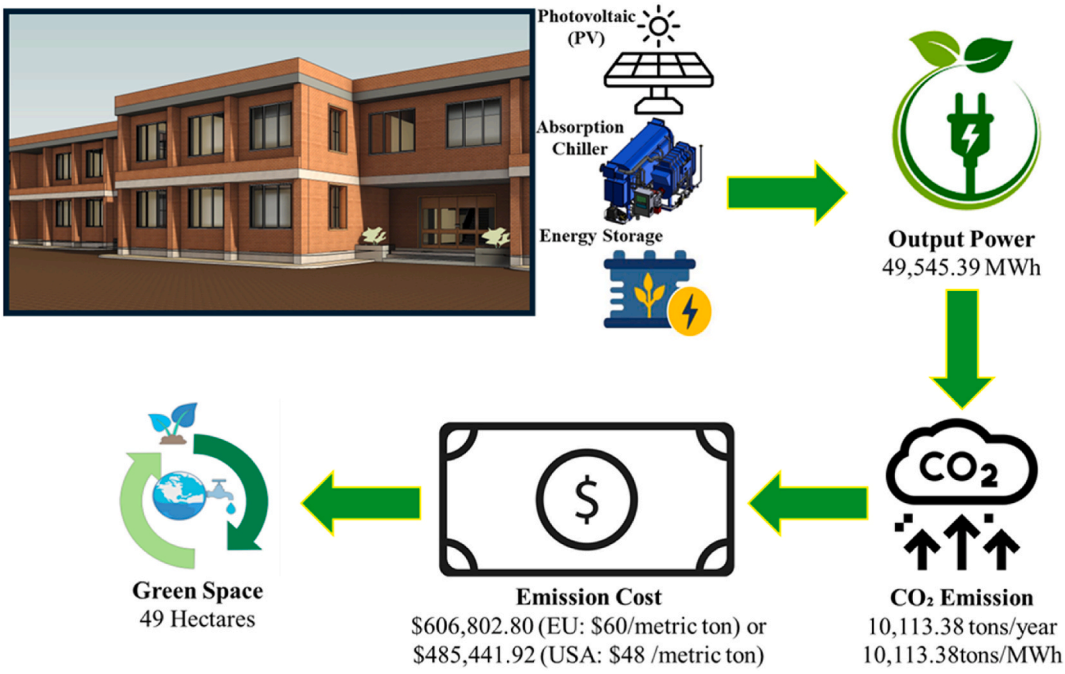

Fig. 17. Environmental benefits of the optimized multi-generation system.

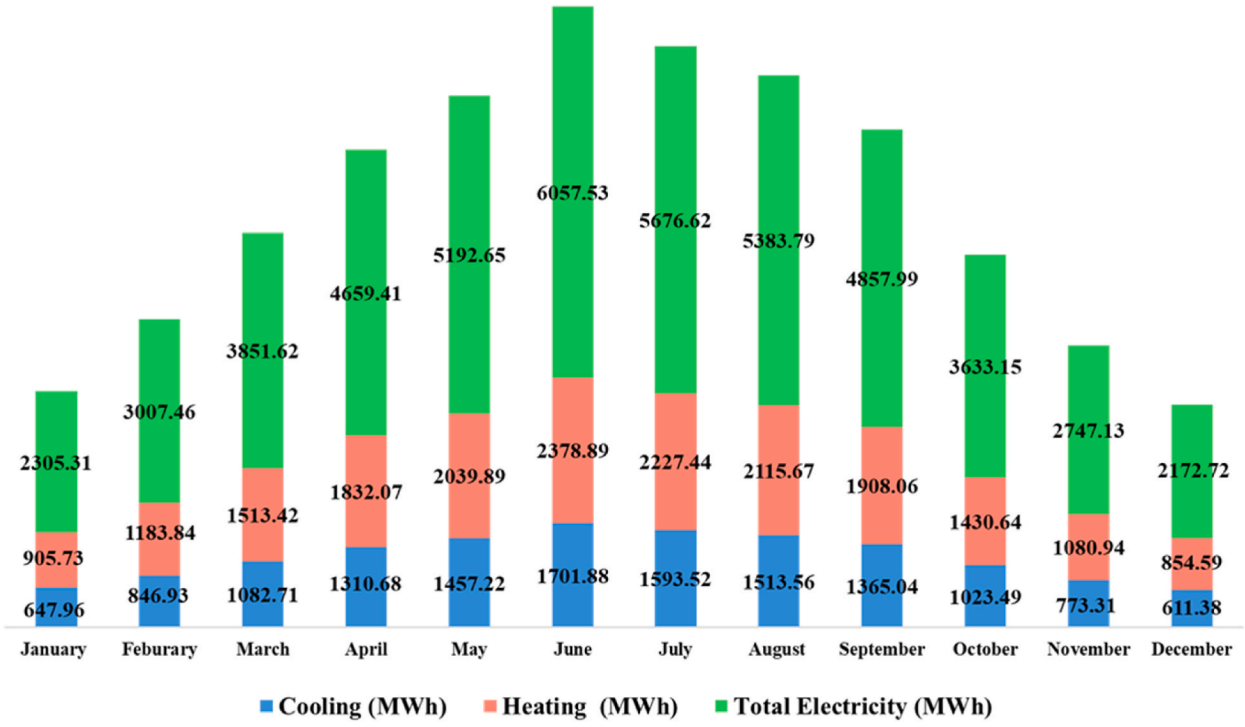

Fig. 18. Total monthly cooling, heating, and electricity generation by the optimized solar farm.

electricity generation, demonstrating seasonal variations in energy production. Cooling output increases significantly from winter to summer, peaking at 2378.89 MWh in June, aligning with the high cooling demand during extreme summer temperatures. Conversely, heating output follows an inverse trend, reaching 2227.44 MWh in July, as the chiller operates in heat recovery mode to repurpose waste heat. Total electricity generation peaks at 6057.53 MWh in June, following the same seasonal pattern. This dynamic balance

ensures efficient system performance by matching cooling and heating production with available solar power. The integration of solar energy with the compression chiller optimizes energy utilization, enhances system efficiency, and reduces dependence on external energy sources, demonstrating a sustainable and self-sufficient multi-generation system designed to meet the energy demands of the case study building.

Fig. 19 illustrates the total monthly cooling demand, cooling generation, and stored cooling energy across the year, demonstrating the system's ability to balance energy supply and demand. During the peak summer months of June and July, cooling generation reaches 1701.88 MWh and 1593.52 MWh, respectively, aligning with high cooling demand (983.92 MWh in June and 1169.70 MWh in July). Even during the highest cooling demand, a portion of the generated cooling energy is still stored, demonstrating the system's resilience and capacity to maintain energy reserves despite increased consumption. The surplus cooling energy (717.95 MWh in June and 423.82 MWh in July) is efficiently stored, ensuring an uninterrupted cooling supply. Conversely, in winter (January and December), when cooling demand is minimal (13.00 MWh and 26.48 MWh, respectively), the system still generates cooling energy (647.96 MWh in January and 611.38 MWh in December), leading to surplus storage (634.96 MWh in January and 584.90 MWh in December). These findings demonstrate that the integration of cooling storage can significantly reduce reliance on external energy sources while maintaining thermal comfort. This highlights the feasibility of self-sustaining renewable energy solutions for climate-adaptive building operations.

Fig. 20 shows the total monthly heating demand, heating generation, and stored heating energy throughout the year. Heating demand remains minimal, peaking at 2.71 MWh in January and 2.27 MWh in December, while demand is zero from March to November due to the warm climate. Despite this, the system continues to generate heating energy, with the highest production in June (2378.89 MWh) and July (2227.44 MWh) when heat recovery processes are maximized. The significant surplus heating generation is stored during these months, ensuring efficient thermal energy utilization. This surplus storage plays a crucial role in maintaining a self-sufficient and energy-resilient system, as stored heat can be redirected for future use, reducing reliance on external heating sources.

Fig. 21 indicates the total monthly electricity demand, electricity generation, and stored electricity across the year, demonstrating the system's ability to manage supply and demand effectively. Electricity demand, which includes lighting and other loads, follows a seasonal pattern, peaking at 1891.19 MWh in July and reaching its lowest level in January (838.32 MWh). Meanwhile, total electricity generation is significantly higher, with a peak output of 6057.53 MWh in June, ensuring a surplus that is stored for later use (4397.50 MWh in June). Even during months of lower demand, such as January (838.32 MWh) and December (860.70 MWh), electricity generation remains high (2305.31 MWh and 2172.72 MWh, respectively), leading to substantial storage (1466.99 MWh in January and 1312.02 MWh in December). These results highlight the effectiveness of the solar-powered multi-generation system in ensuring energy resilience by balancing electricity production and consumption throughout the year. The ability to store surplus electricity further reduces dependency on external energy sources and enhances the reliability of renewable power integration.

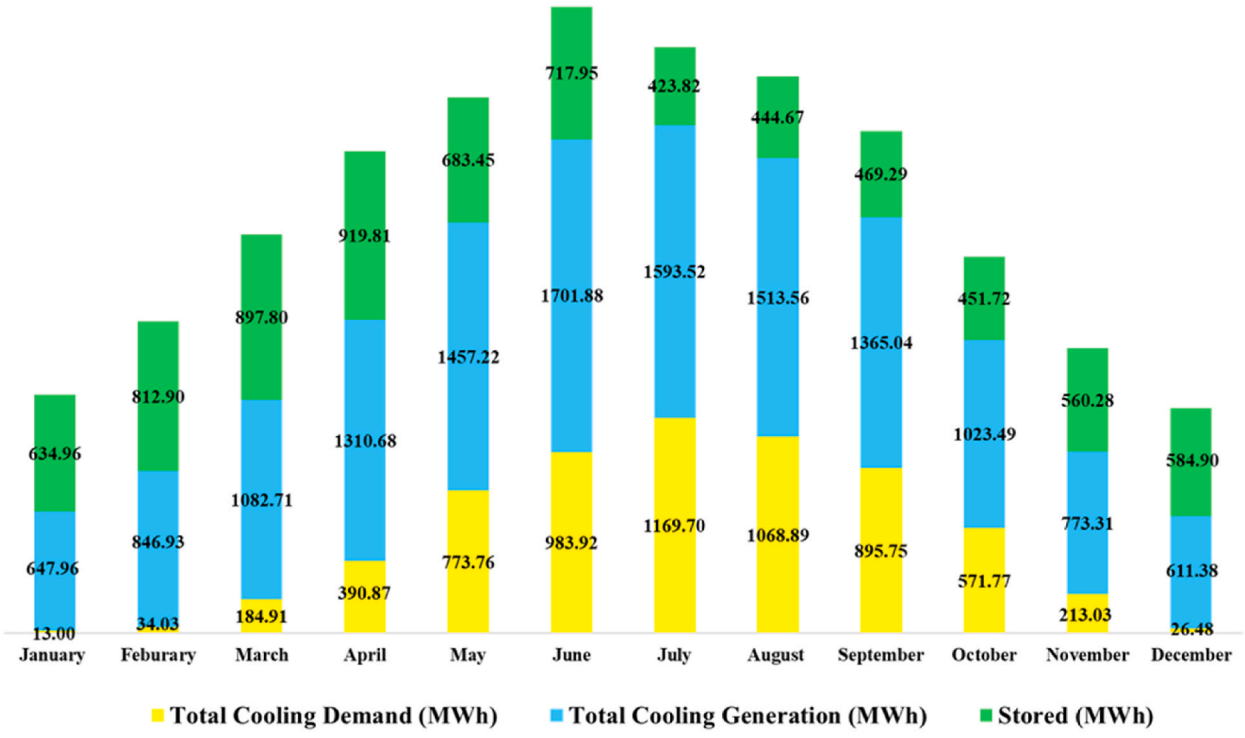

Fig. 19. Monthly cooling demand, generation, and storage in the optimized case.

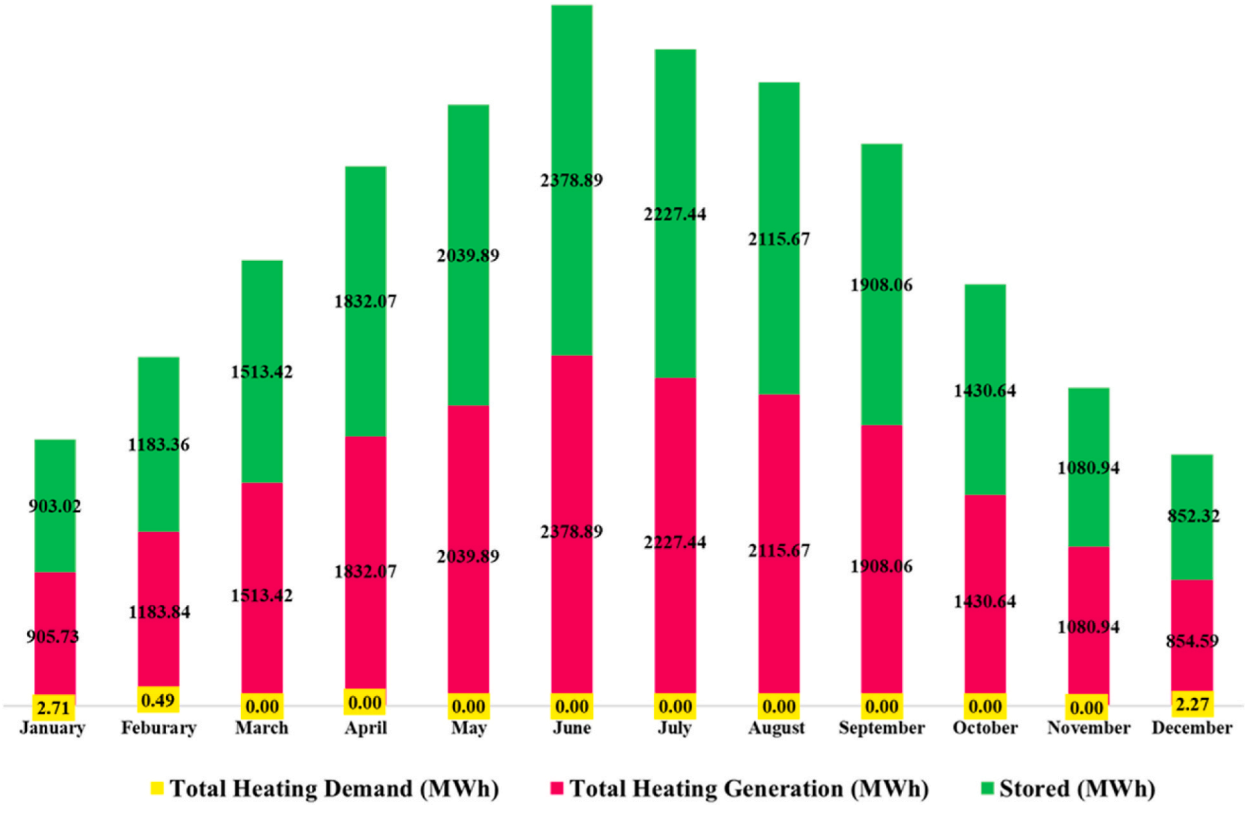

Fig. 20. Monthly heating demand, generation, and storage in the optimized case.

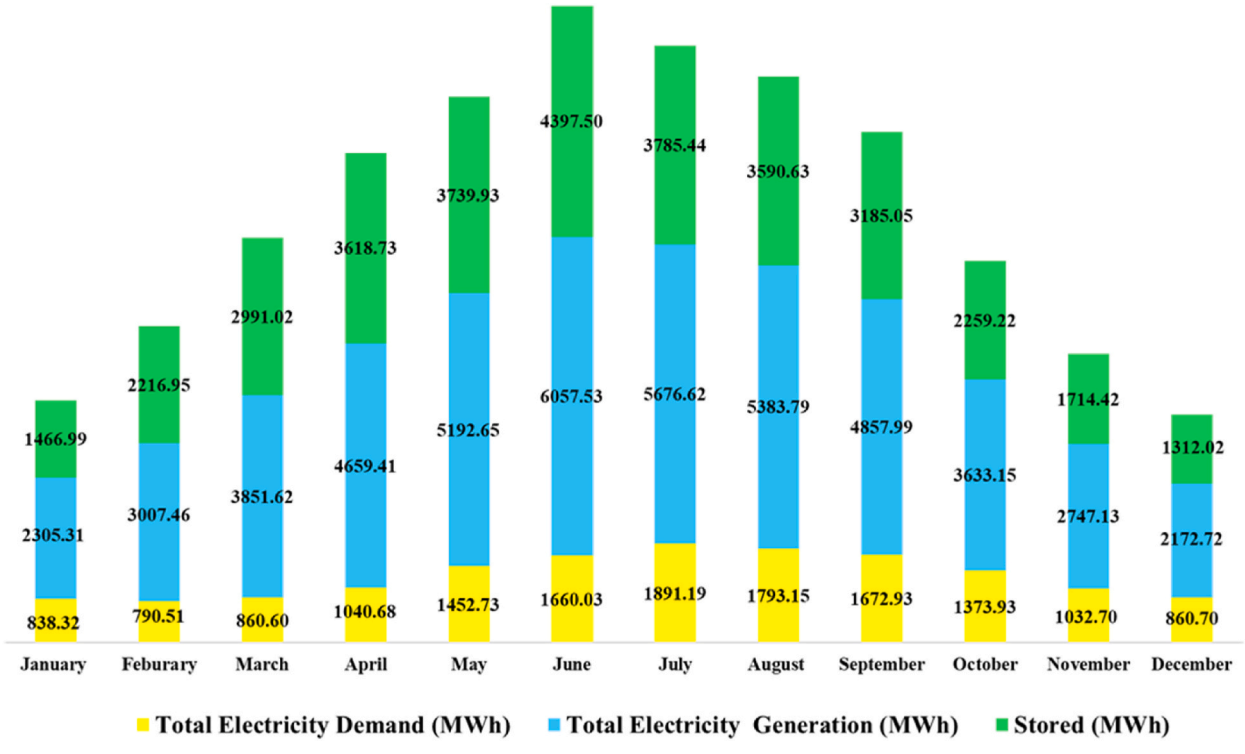

Fig. 21. Monthly heating demand, generation, and storage in the optimized case.

4.4. Comparison of the optimized system with the base case study

This section evaluates the performance improvements achieved through optimization by comparing the optimized solar-powered multi-generation system with the base case, which also incorporates a multi-generation system. The optimization efforts aimed to enhance energy production, efficiency, and sustainability while managing operational costs and environmental impact. Table 9 lists the key performance metrics for both the base case and optimized system, highlighting improvements in electricity production, heating and cooling output, exergy efficiency, operational costs, and environmental impact.

Table 9 indicates that the optimization process resulted in a substantial increase in total electricity production, rising by 224.52 %, demonstrating the system's enhanced capacity to meet the university campus's energy needs while generating a surplus of 34.28 GWh for potential grid export. This surplus energy not only strengthens the institution's energy security but also presents opportunities for financial returns. Heating and cooling outputs have also significantly improved, with heating increasing from 5.5 MWh to 19,470 MWh, a remarkable rise, while cooling output has increased by 120.16 %, from 6326.1 MWh to 13,927.7 MWh over a year. These results highlight the system's ability to efficiently provide both thermal and electrical energy, ensuring year-round indoor comfort while reducing reliance on external energy sources. Despite this, a slight decline in exergy efficiency from 25.69 % to 23.44 % is observed, likely due to increased system complexity and energy throughput, which introduce additional inefficiencies. However, these trade-offs are outweighed by the significant improvements in overall energy performance, with the system now operating at a greater capacity and resilience. The operational cost has increased from $10.15/hour to $14.92/hour, reflecting the expanded scale and performance of the system. Nevertheless, the large surplus electricity generation can offset these costs by reducing dependence on grid electricity or by enabling energy sales, improving the system's long-term economic feasibility.

The optimized solar-powered multi-generation system presents a scalable and sustainable solution for university campuses and other large-scale facilities. Its ability to generate and store surplus energy further strengthens both its economic and environmental benefits, making it a feasible model for cost-effective and energy-efficient campus management. The optimized system contributes to environmental sustainability by reducing CO_2 emissions from 37.18 to 35.34 metric tons/year for the three-story faculty building. While the reduction is modest, the increased reliance on renewable energy sources ensures long-term carbon footprint mitigation. The LCC ($) has increased slightly from 224,315.6 to 239,571.3, a reasonable trade-off considering the enhanced energy production and cost savings from reduced grid dependency. Moreover, the optimized system's potential for surplus energy utilization enhances its long-term financial viability, reinforcing its role as a practical pathway toward energy resilience and sustainability in university campuses.

4.5. Scalability and system flexibility

The optimized solar-powered multi-generation system exhibits significant scalability, making it suitable for various building typologies, including university campuses, commercial complexes, and residential communities. The methodology incorporates demand-side and supply-side optimization, ensuring adaptability to different energy consumption patterns. The modular approach in energy demand optimization, which includes material selection, climatic data analysis, and energy load calculation, allows flexible adjustments based on specific site conditions, occupancy levels, and thermal properties. The use of BEopt software enables iterative refinement of design parameters to suit varying climatic conditions and energy efficiency goals, while EES ensures thermodynamic efficiency across different scales. Importantly, the ANN-GA optimization framework is inherently adaptable to buildings with diverse thermal characteristics, such as varying heat capacities, and to a wide range of climatic conditions. By retraining the neural network with site-specific climate data, material properties, and occupancy patterns, the system can be fine-tuned for different operational scenarios. This adaptability ensures that the proposed energy management strategy is not restricted to hot climates but can be extended effectively to temperate, cold, or mixed climates, supporting its broader application in diverse built environments.

The developed ANN-GA optimization framework exhibits a wide scope of applicability. Provided that the model is retrained using appropriate site-specific climatic data and building operational parameters, it can be effectively applied not only in hot semi-arid regions but also in moderate and colder climates. This adaptability enables the optimization of building energy performance across a broad spectrum of environmental conditions, ensuring the system's relevance for diverse geographic contexts.

Beyond scalability, the system offers high operational flexibility through AI-based optimization using ANN and GA. The ANN model allows the system to dynamically adjust its operation based on real-time energy demands. The GA refines these predictions by optimizing multiple objectives, including efficiency, cost, and emission reductions. This adaptive framework enables automatic

Table 9
Comparison of energy and cost performance in base and optimized multi-generation system.

Parameter	Unit	Base Case	Optimized Case
Cooling Output	GWh/Year	6326.1	13.93
Heating Output	GWh/Year	5.5	19.47
Total Electricity Production	GWh/Year	15,267.5	49.55
Surplus Electricity	GWh/Year	4.56	34.28
Exergy Efficiency	%	25.69	23.44
Operational Cost	$/hour	10.15	14.92
CO_2 Emissions	Metric tons/yr	37.18	35.34
LCC	$	224,315.6	239,571.3

reconfiguration of energy generation and distribution, ensuring optimal performance under varying weather conditions, load demands, and operational constraints. These capabilities establish the proposed system as a resilient, scalable, and future-ready solution for achieving energy efficiency and sustainability in diverse built environments.

4.6. Performance benchmarking against existing systems

This section compares the performance of the optimized solar-powered multi-generation system developed in this study with previous works employing various renewable energy-based optimization approaches. Table 10 lists different optimized multi-generation systems, their respective optimization methods, and key performance metrics.

Table 10 indicates that the proposed system achieves a significantly higher cooling energy compared to almost all benchmarked multi-generation studies, except for offshore renewable systems, which generate substantial cooling energy due to large-scale integration [85]. The proposed system also demonstrates an improved heating output, surpassing all the other systems. The optimized system power output (49,545.4 MWh) is also one of the highest among comparable systems, indicating the system's capability to support extensive energy demands in a university campus setting. The only systems with greater outputs are the solar-driven multi-generation system with an absorption chiller [81] and the offshore renewable system [85], both of which benefit from large-scale integration or alternative energy sources. Despite its high energy generation, the proposed system maintains a competitive exergy efficiency (35.34 %), which is lower than the intelligent solar cogeneration system (44.9 %) [51] but closely aligned with high-performance systems such as the hybrid geothermal-solar multi-generation model (37 %) [80] and the solar-driven absorption chiller system (35.30 %) [81]. These findings highlight the effectiveness of the optimization approach in enhancing system performance while balancing energy efficiency and scalability.

5. Limitations and future work

This study assumes steady-state conditions, which exclude transient variations in weather, occupancy patterns, and energy demand, potentially limiting real-world applicability. Dust accumulation on PV panels, a factor affecting efficiency, particularly in arid and polluted environments, was not considered. Constant convective heat transfer coefficients were also applied, without accounting for wind-induced variations in ambient conditions. The exclusion of radiation exchange at the back of the PV panels assumes minimal heat loss, potentially leading to an underestimation of thermal inefficiencies. The model treated energy transfer as a quasi-steady-state process, which meant it didn't fully account for the system's dynamic behavior of energy storage systems that influence peak demand management and night-time operation. On the economic side, financial cost calculations were based on a fixed average electricity price, without considering dynamic pricing mechanisms such as net-billing tariffs. Furthermore, the environmental assessment focused only on operational emissions, without including embodied carbon emissions associated with the building's full life cycle.

To address these limitations, future studies should integrate transient thermal modeling using TRNSYS or EnergyPlus to capture real-time system behavior and improve accuracy. Dust accumulation effects could be addressed through the development of self-cleaning PV surfaces or predictive maintenance strategies. Incorporating adaptive convective heat transfer models would improve

Table 10
Comparison of the optimized system with previous studies.

Ref	System Description	Optimization Method	Cooling (MWh)	Heating (MWh)	Electricity (MWh)	Exergy Efficiency (%)
Current Study	Optimized solar-powered multi-generation	ANN and GA	13,927.7	19,470	49,545.4	35.34
[80]	Hybrid geothermal-solar multi-generation	Data-driven optimization	113.03	–	276.72	37
[81]	Solar-driven multi-generation with absorption chiller	NSGA-II multi-objective optimization	–	9.628	254,744	35.30
[82]	Integrated geothermal ORC-based with electrolysis & desalination	ANN and GA	67.02 (converted from 7.65 MW)	–	14,730 (MW converted to MWh)	29.69
[83]	Solar-integrated co-generation	BEopt-based optimization	215.3	500	210	25.1
[84]	Solar thermal-powered refrigeration	Multi-objective optimization	473.04 (converted from 54 kWh)	–	175.2 (converted from 20 kWh)	8.7
[55]	Solar-powered multi-generation	Multi-objective optimization (BEopt & EES)	183.37	467.95	166.16	25.18
[85]	Multi-energy complementary offshore renewable with hydrogen-ammonia co-generation	Economic analysis & system optimization	546,810	–	33,090	29.10
[51]	Intelligent solar cogeneration	Tri-objective optimization (ML & GA)	8.85 (converted from 1.01 kWh)	11.99 (converted from 1.37 kWh)	–	44.9

the accuracy of thermal performance predictions by accounting for wind variations. Enhancing the optimization framework with dynamic weather and operational data would further increase system responsiveness and reliability. In terms of economic modeling, future research should consider dynamic electricity pricing models, including time-of-use rates and net-billing mechanisms, to better reflect real-world financial performance. Finally, adopting a full LCC assessment approach is recommended to capture embodied carbon emissions, providing a more comprehensive evaluation of the environmental impact of the proposed energy system.

6. Conclusion

To address the high energy demands and environmental challenges of university buildings, this study developed and optimized a solar-powered multi-generation system using Artificial Neural Networks and Genetic Algorithms for enhanced efficiency and cost-effectiveness. The findings demonstrate that AI-driven optimization can significantly improve energy performance while balancing operational costs and sustainability. Key findings include:

- The optimized system produces 49.55 GWh of electricity annually, far exceeding the university's energy demand. This surplus can reduce dependence on external energy sources, improve grid integration strategies, and provide financial opportunities for surplus energy utilization.
- By increasing heating output from 5.5 MWh to 19.47 GWh and cooling output from 6326.1 MWh to 13.93 GWh, the system ensures a stable and efficient energy supply for year-round thermal comfort. This highlights the role of multi-generation systems in improving building energy resilience while reducing peak load reliance on conventional heating and cooling methods.
- Although exergy efficiency decreased from 25.69 % to 23.44 % compared to the base case, this trade-off reflects the increased energy throughput and expanded system scale. This highlights the need for adaptive control strategies in future systems to maximize efficiency while maintaining high energy output.
- While operational costs increased from $10.15 $/h to 14.92 $/h due to higher system capacity, the substantial surplus electricity offsets expenses, improving the long-term financial viability of the system. CO_2 emissions were also reduced from 37.18 to 35.34 metric tons/year, demonstrating the environmental benefits in institutional settings.
- This study is among the first to integrate an approach combining building energy simulation, thermodynamic validation, and multi-objective optimization using AI in a unified framework for campus-scale multi-generation systems in extreme climates, addressing both operational performance and economic viability.
- High correlation coefficients ($r = 0.97957$ for cost rate and $r = 0.99731$ for exergy efficiency) indicate excellent agreement between predicted and actual values, confirming the accuracy of the ANN-GA optimization framework. Residual analysis showed that most prediction errors were small and normally distributed, while empirical validation against published solar data further confirmed the reliability and generalizability of the model.

Overall, this research shows that AI-driven multi-generation systems can be adapted for larger-scale use, from industrial settings to district-wide energy networks. Future research should focus on integrating real-time weather data, dynamic energy forecasting, and hybrid renewable solutions to enhance system resilience, adaptability, and economic feasibility in complex energy infrastructures.

CRediT authorship contribution statement

Ehsanolah Assareh: Writing – original draft, Visualization, Validation, Methodology, Investigation, Formal analysis, Data curation, Conceptualization, Software. **Nima Izadyar:** Writing – review & editing, Writing – original draft, Visualization, Supervision, Project administration, Methodology, Investigation, Formal analysis. **Elmira Jamei:** Writing – review & editing, Resources, Investigation. **Mohammad amin Monzavian:** Writing – review & editing, Software, Data curation. **Saurabh Agarwal:** Writing – review & editing, Writing – original draft, Formal analysis, Data curation, Conceptualization. **Neha Agarwal:** Writing – review & editing, Writing – original draft, Validation, Supervision, Formal analysis, Data curation.

Declaration of Generative AI

During the preparation of this work, the authors used an OpenAI tool to enhance language and readability. After using the tool, the authors reviewed and edited the content as needed. They take full responsibility for the final content of the publication. The authors highlight that AI's role was to assist in refining the text and language, and not to replace any critical tasks of the authors.

Declaration of competing interest

The authors confirm that the work described in this manuscript has not been published previously. The article is not under consideration for publication elsewhere, and its publication has been approved by all authors and the responsible authorities at the institutions where the work was carried out. If accepted, this article will not be published elsewhere in the same form, in English, or in any other language, including electronically, without the written consent of the copyright holder.

We confirm adherence to our institutes' intellectual property guidelines and affirm that no IP constraints delay publication. All authors involved in the preparation of this manuscript are recognized, and the order of authors listed in the manuscript has been approved by all authors, following their relative contributions.

After a thorough investigation, the authors have disclosed all potential conflicts of interest and have found none associated with this publication. The authors declare that they have no competing financial or personal interests that could have influenced the work reported in this manuscript. This research has not received any external funding.

AI-assisted technologies were used to improve language and readability, and a separate section titled “Declaration of Generative AI” has been included in the manuscript, as per the journal’s guidelines. After using AI, the authors reviewed and edited the content as needed. They take full responsibility for the content of the published article.

This declaration is submitted as part of the revised manuscript (**Ref No**: JBE-D-25-03315) following peer review.

The corresponding author is the main contact for the Editorial process and is responsible for communicating with the other authors about progress, revisions, and final approval of proofs.

Data availability

Data will be made available on request.

References

[1] F. Birol, World Energy Outlook 2022, International Energy Agency, Paris, France, 2022, p. 522.
[2] IEA, World Energy Outlook 2024, 2024.
[3] Y. Qin, et al., Pearson correlation analysis between carbon dioxide emissions and socioeconomic factors across nations’ income groups, Chem. Eng.Transac. 106 (2023) 181–186.
[4] T.S. Kabel, M. Bassim, Reasons for shifting and barriers to renewable energy: a literature review, Int. J. Energy Econ. Pol. 10 (2) (2020) 89–94.
[5] B. Elias, Towards Best Practices for Historic Retrofits: Tradeoffs for Historic Buildings’ Operating Energy Retrofits, Columbia University, 2021.
[6] B. Wu, R. Maalek, Renovation or redevelopment: the case of smart decision-support in aging buildings, Smart Cities 6 (4) (2023) 1922–1936.
[7] S. Pierce, et al., District energy modelling for decarbonisation strategies development—the case of a University campus, Energy Rep. 11 (2024) 1256–1267.
[8] IEA, World Energy Outlook 2024 - Free Dataset, I.E.A, IEA, 2024.
[9] R.A. Almasri, N.H. Abu-Hamdeh, N. Al-Tamimi, A state-of-the-art review of energy-efficient and renewable energy systems in higher education facilities, Front. Energy Res. 11 (2024) 1344216.
[10] J. Ge, et al., Energy efficiency optimization strategies for university research buildings with hot summer and cold winter climate of China based on the adaptive thermal comfort, J. Build. Eng. 18 (2018) 321–330.
[11] N.T. Hung, Data-driven predictive models for daily electricity consumption of academic buildings, Aims Energy 8 (5) (2020).
[12] A. Sretenovic, Analysis of Energy Use at University Campus, Institutt for energi-og prosessteknikk, 2013.
[13] K. Gjoka, B. Rismanchi, R.H. Crawford, Fifth-generation district heating and cooling: opportunities and implementation challenges in a mild climate, Energy 286 (2024) 129525.
[14] J.P. Laporte, J.M. Cansino, Energy consumption in higher education institutions: a bibliometric analysis focused on scientific trends, Buildings 14 (2) (2024) 323.
[15] T. Quevedo, et al., Benchmarking energy consumption in universities: a review, J. Build. Eng. 82 (2024) 108185.
[16] K. Arshad, et al., Air pollution and climate change as grand challenges to sustainability, Sci. Total Environ. (2024) 172370.
[17] IEA, The breakthrough agenda report, in: *THE BREAKTHROUGH AGENDA REPORT* 2024, INTERNATIONAL ENERGY AGENCY (IEA), 2024.
[18] U. Unep, 2022 Global Status Report for Buildings and Construction, International Energy Agency and the United Nations Environment Programme (UNEP), 2019.
[19] Y. Li, B. Wang, Y. Fei, Green renovation of building envelopes in higher education institutions: study of energy-saving and carbon reduction at Nanjing audit university Mochou campus, Int. J. Low Carbon Technol. 20 (2025) 1057–1079.
[20] E.K.A. Ahmed, et al., An integrated framework for sustainable retrofitting of existing university buildings, Discover Sustain. 6 (1) (2025) 38.
[21] R.K. Jaysawal, et al., Concept of net zero energy buildings (NZEB)-A literature review, Clean. Eng. Technol. 11 (2022) 100582.
[22] H.-L. Lou, S.-H. Hsieh, Towards zero: a review on strategies in achieving net-zero-energy and net-zero-carbon buildings, Sustainability 16 (11) (2024) 4735.
[23] D.H. Li, L. Yang, J.C. Lam, Zero energy buildings and sustainable development implications–A review, Energy 54 (2013) 1–10.
[24] W. Zhang, et al., A critical review of the performance evaluation and optimization of grid interactions between zero-energy buildings and power grids, Sustain. Cities Soc. 86 (2022) 104123.
[25] S.K. Singh, A.K. Tiwari, Solar-powered hydrogen production: advancements, challenges, and the path to net-zero emissions, Int. J. Hydrogen Energy 84 (2024) 549–579.
[26] N.S.M.N. Izam, et al., Sustainable development perspectives of solar energy technologies with focus on solar Photovoltaic—a review, Energies 15 (8) (2022) 2790.
[27] A.O. Maka, J.M. Alabid, Solar energy technology and its roles in sustainable development, Clean Energy 6 (3) (2022) 476–483.
[28] S. Di Fraia, et al., Solar-based systems, in: Polygeneration Systems, Elsevier, 2022, pp. 193–237.
[29] M.R. Sharifinasab, S. Khanmohammadi, Exergo-economic analysis and AI optimization of a conceptual multi-level solar-driven system for building application, J. Build. Eng. 100 (2025) 111667.
[30] S. Sami, M. Gholizadeh, M. Deymi-Dashtebayaz, An applicable multi-generation system for different climates from energy, exergy, exergoeconomic, economic, and environmental (5E) perspectives, Sustain. Cities Soc. 100 (2024) 105057.
[31] E. Baniasadi, et al., Exergy-economic analysis of a solar-geothermal combined cooling, heating, power and water generation system for a zero-energy building, Int. J. Hydrogen Energy 48 (99) (2023) 39064–39083.
[32] M. Noro, S. Mancin, R. Riehl, Energy and economic sustainability of a trigeneration solar system using radiative cooling in mediterranean climate, Sustainability 13 (20) (2021) 11446.
[33] A. Ye, et al., Using solar energy to achieve near-zero energy buildings in Tibetan Plateau, Renew. Energy 218 (2023) 119347.
[34] E. Kyriaki, E. Giama, Hybrid solar photovoltaic thermal systems in Nearly-Zero Energy Buildings: the case of a residential building in Greece, Int. J. Sustain. Energy 41 (10) (2022) 1521–1532.
[35] S. Ahmadi, et al., Design and evaluation of renewable energies-based multi-generation system for hydrogen production, freshwater and cooling, Renew. Energy 198 (2022) 916–935.
[36] S. Sarvar-Ardeh, et al., Recent advances in the applications of solar-driven co-generation systems for heat, freshwater and power, Renew. Energy (2024) 120256.
[37] M.A. Kabir, et al., Sustainable energy transition in Bangladeshi academic buildings: a techno-economic analysis of photovoltaic-based net zero energy systems, Energy Build. 312 (2024) 114205.
[38] C. Munguba, et al., Enhancing cost-efficiency in achieving near-zero energy performance through integrated photovoltaic retrofit solutions, Appl. Energy 367 (2024) 123307.
[39] P. Fonseca, et al., Sustainability in university campus: options for achieving nearly zero energy goals, Int. J. Sustain. High Educ. 19 (4) (2018) 790–816.
[40] X. Luo, L.O. Oyedele, Integrated life-cycle optimisation and supply-side management for building retrofitting, Renew. Sustain. Energy Rev. 154 (2022) 111827.

[41] K. Mohammadi, et al., A comprehensive review of solar only and hybrid solar driven multigeneration systems: classifications, benefits, design and prospective, Appl. Energy 268 (2020) 114940.
[42] M. Ibrahim, et al., Building retrofitting towards net zero energy: a review, Energy Build. 322 (2024) 114707.
[43] F. Abdel-Jaber, K.N. Dirks, A review of cooling and heating loads predictions of residential buildings using data-driven techniques, Buildings 14 (3) (2024) 752.
[44] B.P. Raj, et al., A review on numerical approach to achieve building energy efficiency for energy, economy and environment (3E) benefit, Energies 14 (15) (2021) 4487.
[45] M.E. Yıldız, F. Beyhan, Prediction of cooling load via machine learning on building envelope design parameters, J. Build. Eng. 100 (2025) 111724.
[46] K.A. Barber, M. Krarti, A review of optimization based tools for design and control of building energy systems, Renew. Sustain. Energy Rev. 160 (2022) 112359.
[47] S.A. Muslim, EnergyPlus-Towards the selection of right simulation tool for building energy and power systems research, J. Energy. Power Technol. 3 (3) (2021) 1–9.
[48] O.M. Mbayam, T. Bounahmidi, Energy optimization of a residential building for electricity, cooling, and heating: a path to Net Zero Energy, Energy Sustain. Dev. 85 (2025) 101672.
[49] B. McPherson-Hathaway, Comparing BEopt (EnergyPlus) Energy Predictions to Measured Circuit Level Energy Consumption of 12 Similar Small Energy-Efficient Single-Family Residences, 2021.
[50] A. Izadi, et al., Transient simulation and techno-economic assessment of a near-zero energy building using a hydrogen storage system and different backup fuels, Int. J. Hydrogen Energy 47 (74) (2022) 31927–31940.
[51] B. Saadmohammadi, B. Sajadi, 4E analysis and tri-objective optimization of a novel solar 4th cogeneration system for a smart residential building in various climates of Iran, Energy Convers. Manag. 303 (2024) 118177.
[52] F. Johari, et al., Towards urban building energy modelling:: a comparison of available tools, in: eceee 2019 Summer Study on energy efficiency: Is efficient sufficient?, 3–8 June, Presqu'île de Giens, Hyères, France, 2019.
[53] B.B.B.E.O. Tool, 5 best energy modeling software tools for net-zero buildings: digital architects of sustainability, Energy (2024), 0.
[54] C. Christensen, et al., BEopt (TM) Software for Building Energy Optimization: Features and Capabilities, National Renewable Energy Lab.(NREL), Golden, CO (United States), 2006.
[55] E. Assareh, N. Agarwal, M. Lee, Zero energy building optimization for a residential complex with a new optimized cogeneration system for electricity, cooling, heating and freshwater production, Appl. Therm. Eng. 244 (2024) 122527.
[56] V. Bakırcıoğlu, H.B. Jond, F. Yilmaz, Multi-Objective optimization and thermodynamic analysis of a supercritical CO2 Brayton cycle in a solar-powered multigeneration plant for net-zero emission goals, Energy Convers. Manag. 328 (2025) 119628.
[57] D. Cai, et al., Cost and thermodynamic analysis of wind-hydrogen production via multi-energy systems, Energy Convers. Manag. 306 (2024) 118286.
[58] A. Nikitin, et al., Energy, exergy, economic and environmental (4E) analysis using a renewable multi-generation system in a near-zero energy building with hot water and hydrogen storage systems, J. Energy Storage 62 (2023) 106794.
[59] E. Assareh, et al., Optimization of solar farm design for energy efficiency in university campuses using machine learning: a case study, Eng. Appl. Artif. Intell. 153 (2025) 110847.
[60] C. Yılmaz, O. Sen, Feasibility of optimum energy use and cost analyses by applying artificial intelligence and genetic optimization methods in geothermal and solar energy-assisted multigeneration systems, Renew. Energy (2024) 121548.
[61] H. Hajabdollahi, et al., Evaluation & optimization of solar-fossil-fuel-based multi-generation system with energy storage, Appl. Therm. Eng. 245 (2024) 122682.
[62] I. Din, M.A. Rosen, P. Ahmadi, Optimization of Energy Systems, John Wiley & Sons, 2017.
[63] M. Ibnouf, et al., A comprehensive review of AI algorithms for performance prediction, optimization, and process control in desalination systems, Desalination Water Treat. (2024) 100892.
[64] F. Rong, et al., Performance evaluation and multi-objective optimization of hydrogen-based integrated energy systems driven by renewable energy sources, Energy 313 (2024) 133698.
[65] E. Assareh, et al., Application of a multi-objective approach integrating solar-wind co-generation with response surface method to optimize zero-energy buildings, Appl. Therm. Eng. (2025) 125637.
[66] E. Assareh, et al., Optimizing solar photovoltaic farm-based cogeneration systems with artificial intelligence (AI) and Cascade compressed air energy storage for stable power generation and peak shaving: a Japan-focused case study, Appl. Energy 377 (2025) 124468.
[67] S. Mobayen, et al., Multi-functional hybrid energy system for zero-energy residential buildings: integrating hydrogen production and renewable energy solutions, Int. J. Hydrogen Energy 102 (2025) 647–672.
[68] Y. Lin, et al., Advancing AI-enabled techniques in energy system modeling: a review of data-driven, mechanism-driven, and hybrid modeling approaches, Energies 18 (4) (2025) 845.
[69] M.M. Forootan, et al., Machine learning and deep learning in energy systems: a review, Sustainability 14 (8) (2022) 4832.
[70] T.M. Alabi, et al., A review on the integrated optimization techniques and machine learning approaches for modeling, prediction, and decision making on integrated energy systems, Renew. Energy 194 (2022) 822–849.
[71] V.R. Ravipudi, H.S. Keesari, Design Optimization of Renewable Energy Systems Using Advanced Optimization Algorithms, Springer Nature, 2022.
[72] F. Ren, Z. Wei, X. Zhai, A review on the integration and optimization of distributed energy systems, Renew. Sustain. Energy Rev. 162 (2022) 112440.
[73] A. Konak, D.W. Coit, A.E. Smith, Multi-objective optimization using genetic algorithms: a tutorial, Reliab. Eng. Syst. Saf. 91 (9) (2006) 992–1007.
[74] A. Parifard, A. Naeini, A. Jalali, AI-based optimization of a sustainable system for water, energy, and ventilation supply of a smart residential building, J. Build. Eng. 104 (2025) 112350.
[75] Meteotest. *Meteonorm*: Global meteorological data for any location. [cited 2024 7 October]; Available from: https://meteonorm.com/en/.
[76] E. Bas, E. Egrioglu, T. Cansu, Robust training of median dendritic artificial neural networks for time series forecasting, Expert Syst. Appl. 238 (2024) 122080.
[77] S.A. Sharif, A. Hammad, Developing surrogate ANN for selecting near-optimal building energy renovation methods considering energy consumption, LCC and LCA, J. Build. Eng. 25 (2019) 100790.
[78] M. Mehrpooya, et al., Investigation of a hybrid solar thermochemical water-splitting hydrogen production cycle and coal-fueled molten carbonate fuel cell power plant, Sustain. Energy Technol. Assessments 47 (2021) 101458.
[79] K. Kanyarusoke, J. Gryzagoridis, G. Oliver, Validation of TRNSYS modelling for a fixed slope photovoltaic panel, Turk. J. Electr. Eng. Comput. Sci. 24 (6) (2016) 4763–4772.
[80] M.A. Ismail, et al., Machine learning-based optimization and dynamic performance analysis of a hybrid geothermal-solar multi-output system for electricity, cooling, desalinated water, and hydrogen production: a case study, Appl. Therm. Eng. (2025) 125834.
[81] S. Zhang, et al., Multi-level study on solar-driven polygeneration system with thermal energy storage based on pinch method and multi-objective optimization, Int. J. Hydrogen Energy 106 (2025) 644–661.
[82] M.J.R. Asadabadi, et al., ANN-boosted optimization and performance evaluation of a hybrid solar-geothermal high temperature cascaded ORC for electricity, liquid hydrogen, freshwater, and cooling purposes, Appl. Therm. Eng. 262 (2025) 125251.
[83] E. Assareh, et al., A proposal on a co-generation system accompanied with phase change material to supply energy demand of a hospital to make it a zero energy building (ZEB), Energy Build. 318 (2024) 114478.
[84] B. Karthikeyan, et al., Solar powered cascade system for sustainable deep-freezing and power generation-exergoeconomic evaluation and multi-objective optimization for tropical regions, Therm. Sci. Eng. Prog. 50 (2024) 102552.
[85] Y. Zhao, et al., Performance analysis and multi-objective optimization of the offshore renewable energy powered integrated energy supply system, Energy Convers. Manag. 304 (2024) 118232.